Tectonophysics xxx (2014) xxx–xxx

Contents lists available at ScienceDirect

Tectonophysics

journal homepage: www.elsevier.com/locate/tecto

Crustal deformation styles along the reprocessed deep seismic reflection transect of the Central Iberian Zone (Iberian Peninsula)

Siddique Akhtar Ehsan [a,*], Ramon Carbonell [a], Puy Ayarza [b], David Martí [a], Andrés Pérez-Estaún [a], David Jesús Martínez-Poyatos [c], Jose Fernando Simancas [c], Antonio Azor [c], Luis Mansilla [d]

[a] Department of Structure and Dynamics of the Earth, Institute of Earth Sciences Jaume Almera, ICTJA-CSIC, Lluis Sole i Sabaris s/n, 08028 Barcelona, Spain
[b] Department of Geology, University of Salamanca, 37008 Salamanca, Spain
[c] Department of Geodynamics, Faculty of Science, University of Granada, E-18071 Granada, Spain
[d] School of Industrial Engineering and Mining of Almaden, University of Castilla-La Mancha, Almaden, Spain

ARTICLE INFO

Article history:
Received 30 October 2013
Received in revised form 19 February 2014
Accepted 21 February 2014
Available online xxxx

Keywords:
Deep reflection seismic
Variscan Orogen
Central Iberian Zone
Migration
Crustal structure
Moho discontinuity

ABSTRACT

The multichannel normal incidence (230 km long) deep seismic reflection profile ALCUDIA was acquired in summer 2007. This transect samples an intracontinental Variscan orogenic crust going across, from north to south, the major crustal domain (the Central Iberian Zone) and its suture zone with the Ossa–Morena Zone (the Central Unit) both build up most of the southwestern part of the Iberian Peninsula basement. This high resolution (60–90 fold) profile images about 70 km depth (20 s TWTT) of the continental lithosphere. A new data processing flow provides better structural constraints on the shallow and deep structures resulting in an image that reveals indentation features which strongly suggest horizontal tectonics. The ALCUDIA seismic image shows an upper crust c. 13 km thick decoupled from the comparatively reflective lower crust. The shallow reflectivity of the upper crust can be correlated with surface geological features mapped in the field whereas the deep reflectivity represents inferred imbricate thrust systems and listric extensional faults. The reflectivity of the mid-lower crust is continuous, high amplitude, and horizontal to arcuate though evidences of deformation are present as ductile boudinage structures, thrusting and an upper mantle wedge, suggesting a transpressional flower structure. The image reveals a laminated c. 1.5 km thick, subhorizontal to flat Moho indicating an average crustal thickness of 31–33 km. The Moho shows laterally variable signature, being highly reflective beneath the Central Iberian Zone, but discontinuous and diffuse below the Ossa–Morena Zone. The gravity response suggests relatively high density bodies in the mid-lower crust of the southern half of the transect. The seismic results suggest two major horizontal limits, a horizontal discontinuity at c. 13–15 km (corresponding to the brittle–ductile transition) and the Moho boundary both suggested to act as decoupling surfaces.

1. Introduction

The Iberian Massif is the largest outcrop of the Late Paleozoic Variscan/Alleghanian Orogen in western Europe (Fig. 1a). It was formed by the convergence and collision of the continental plates of Laurentia–Baltica and Gondwana (Franke, 2000; Matte, 2001). The shortening generated by this transpressional collision was mostly accommodated by relatively large and localized deformation belts (suture zones) at the edges of the involved continental domains. In addition, a more distributed deformation zone between sutures accommodates the residual deformation in a typical intra-continental scenario. The structures within the main collision zone are relatively well constrained with the development of well-defined thrusts faults and folds, resulting in the imbrication of the crust at the plate boundaries involved in the collision. These structural features developed mainly depending on the existing stress field coupled with the physical properties and/or lithologies of the crustal units involved in the collision. The Variscan Orogen has been targeted by deep seismic reflection experiments, such as BIRPS (Freeman et al., 1988; Klemperer and Matthews, 1987; Onken et al., 2000), and DEKORP (Carbonell et al., 1996, 1998, 2000; Echtler et al., 1996; Friberg et al., 2002; Juhlin et al., 1998; Tryggvason et al., 2001) through most of the Eurasian continent. In the southwestern part of Iberia the Variscan Orogen was unravelled by the IBERSEIS

Abbreviations: CIZ, Central Iberian Zone; OMZ, Ossa–Morena Zone; SPZ, South Portuguese Zone; CU, Central Unit; TF, Toledo Fault; MF, Mora Fault; MaF, Matachel Fault; AF, Azuaga Fault; UC, Upper crust; MC, Middle crust; LC, Lower crust; DL, Decollement level; HW, Hanging wall; FW, Footwall; DLCR, Dense lower crustal reflectivity; DFWR, Dense footwall reflectivity; VP, Vibroseis point; CDP, Common midpoint; NMO, Normal moveout; DMO, Dip moveout; IRB, IBERSEIS Reflective Body.

* Corresponding author. Tel.: +34 93 4095410; fax: +34 93 4110012.
E-mail addresses: sakhtar@ictja.csic.es (S.A. Ehsan), ramon.carbonell@csic.es (R. Carbonell), puy@usal.es (P. Ayarza), dmarti@ictja.csic.es (D. Martí), andres@ictja.csic.es (A. Pérez-Estaún), djmp@ugr.es (D.J. Martínez-Poyatos), simancas@ugr.es (J.F. Simancas), azor@ugr.es (A. Azor), luis.mansilla@uclm.es (L. Mansilla).

http://dx.doi.org/10.1016/j.tecto.2014.02.014

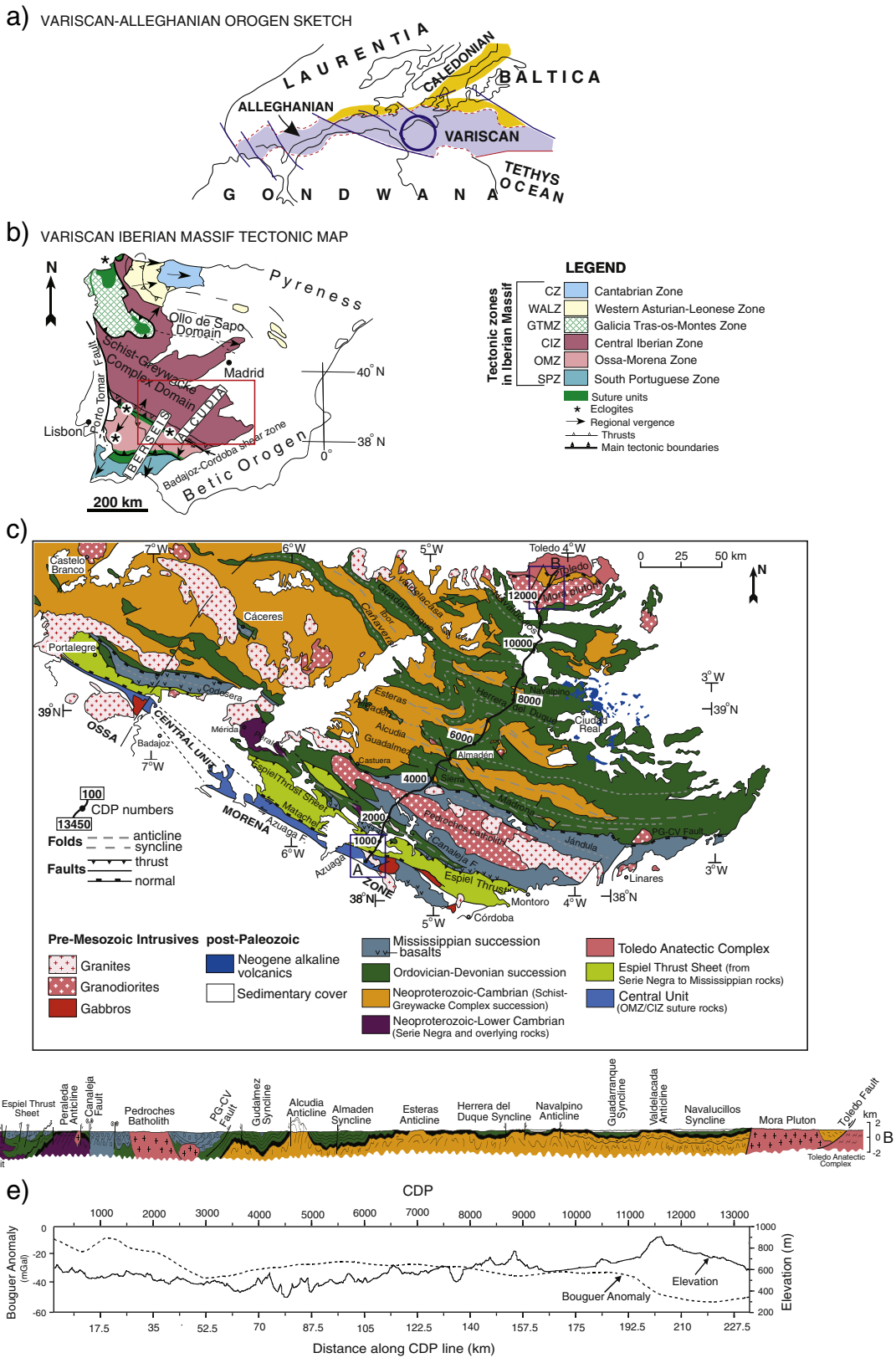

Fig. 1. (a) Sketch illustrating the extension of the Variscan–Alleghanian Orogen. The blue circle indicates the location of the Iberian Massif. (b) The tectonic map of the Iberian Peninsula with the main zones of the Iberian massif and the location of normal incidence deep seismic reflection transects. The red rectangle indicates the location of the study area and it is expanded in (c). (c) Geological map in the survey area showing location of the ALCUDIA deep seismic reflection profile. The blue rectangles at the ends of the ALCUDIA transect are presented in Figs. 5 and 7. The CDPs are indicated along the transect. (d) The structural cross section derived from surface geology. (e) The Bouguer gravity anomaly and the topographic profiles along the ALCUDIA deep seismic reflection profile (modified from Martínez-Poyatos et al., 2012).

Please cite this article as: Ehsan, S.A., et al., Crustal deformation styles along the reprocessed deep seismic reflection transect of the Central Iberian Zone (Iberian Peninsula), Tectonophysics (2014), http://dx.doi.org/10.1016/j.tecto.2014.02.014

experiments (Carbonell et al., 2004; Palomeras et al., 2009; Simancas et al., 2003). However, how the residual deformation is distributed within the interior of the plate is still an unresolved issue. The ALCUDIA (Martínez-Poyatos et al., 2012) deep seismic reflection transect was one of the first attempts to characterize the deformation of a relatively old intracontinental deformed zone far from the known sutures and lacking surface outcrops of localized high or weak strain zones within the crust. In such a tectonic setting the lack of surface exposures of the deep rocks results in little or almost no control/knowledge on the structure beneath the first few kilometres.

The current topography of the Iberian plate is strongly conditioned by the post Variscan plate tectonic evolution during the Mesozoic and the Tertiary (Casas-Sainz and Cortés-Gracia, 2002; Casas-Sainz and Faccenna, 2001; Cloetingh et al., 2002; Rosenbaum et al., 2002; Tejero et al., 2006; Verges and Fernandez, 2006; De Vicente and Vegas, 2009). Long wavelength (hundreds of km) synclinal and anticlinal (sinuous) topography above 700 m in average, characterizes the study area of the Central Iberian Zone (CIZ) and most of the Iberian Plateau. This large scale folding caused differential uplift/subsidence of different areas of the Iberian plate and conditioned the distribution of basins and ranges, bounded by folds and faults, suggesting a lithospheric scale folding (Casas-Sainz and De Vicente, 2009; Cloetingh et al., 2002; De Vicente and Vegas, 2009). However, seismic constraints on the crustal structure from passive and active seismic source experiments (Diaz and Gallart, 2009) suggest that the Moho discontinuity lacks significant topography in the Iberian Plateau. High resolution normal incidence seismic reflection data acquired in the southwestern part of the Iberian Peninsula, namely the IBERSEIS and ALCUDIA transects (Fig. 1b), also reveal a horizontal Moho at, c. 31–33 km depth. This is indicative that, most probably, the recent internal deformation affecting the southwest (caused by compression, collision between Africa and Iberia) of the rigid plate of Iberia is limited and mostly accommodated by structures within the crust.

With these antecedents in mind, the Vibroseis normal incidence transect, ALCUDIA, was reprocessed. Then, an attempt was made to reinterpret the image beyond the primary results by Martínez-Poyatos et al., 2012. The new image improves the resolution of the near surface features allowing a more accurate correlation with the surface geology. It also reveals different seismic reflection fabrics which place some constraints on the stress field and help with the assessment of the internal crustal deformation. The overall image suggests the possibility of crustal flow, such mechanism could account for the inferred decoupling between the topography of the surface and that of the Moho. The reprocessing of the data has improved the quality of reflections by means of a careful choice of processing parameters and an optimal stacking velocity model. The preservation of the true crustal reflectivity and that of steeply dipping structures was also carefully considered. For the first time, a detailed structural interpretation of the upper and lower crust is presented on depth converted migrated sections. The new analysis of the data enabled us (i) to significantly improve the geometry of the principal faults and reflections, (ii) to further constrain the previous geological interpretation by Martínez-Poyatos et al. (2012), and (iii) to update and propose new geological points of views on critical sections along the profile.

2. Tectonic framework

The Iberian Massif is part of the Variscan Orogen of western Europe and the CIZ is a significant continental portion of the Iberian Massif (Fig. 1a and b). The CIZ can be considered the equivalent of the Moldanubian Zone in the Variscan of central Europe (Franke, 2000; Vollbrecht et al., 1989). The Variscan belt was the product of the collision of two continents, Laurentia–Baltica to the north and Gondwana to the south, during the Late Paleozoic (Franke, 2000; Matte, 1986, 2001). Within the Iberian Peninsula the evolution of the Variscan belt has been extensively studied (e.g., Pérez-Estaún and Bea, 2004). A complete cross section of a portion of the orogen actually outcrops in the southwestern part of the peninsula and it was the key target of the IBERSEIS seismic experiment (Carbonell et al., 2004; Simancas et al., 2003). The physical properties of that portion of the orogen have been also constrain by a complementing wide-angle transect (Palomeras et al., 2009, 2010, 2011).

The Variscan Orogen in southwest Iberia is composed of continental blocks (South Portuguese, Ossa–Morena and Central Iberian Zones) bounded by suture units (Fig. 1b). The OMZ is limited to the north by the Badajoz–Cordoba shear zone, which includes the Central Unit (CU); it is recognized as a major suture zone (Azor et al., 1994; Burg et al., 1981; Simancas et al., 2001). The CU is a north dipping continuous ductile shear band 5 km in width. It is bounded by the Azuaga Fault (AF) to the south and the Matachel Fault (Maf) to the north (Fig. 1c and d). The latter is considered to be the southern limit of the CIZ. The ALCUDIA transect samples the CU in its southern end and extends for, approximately 230 km to the north in the CIZ. The surface geology of the CIZ is characterized by, a series of synclinal and anticlinal upright folds and faults NW–SE oriented (Fig. 1c). The CIZ also features igneous intrusions as granitic plutons and batholiths of different sizes (Fig. 1c). ALCUDIA transect crossing a couple of them (Pedroches batholith and Mora pluton). Furthermore, one of the largest mercury mines is located about 100 km north of the southern end of the transect, the Almadén mercury deposit (Jebrak et al., 2002; Saupe, 1990). The Almadén mine has produced over 35% of world's mercury production (Boorder and Westerhof, 1994). The northern end of the transect is located just north of the Toledo Fault (Fig. 1c and d), which is a ductile–brittle extensional shear zone cropping out just south of the city of Toledo (Barbero, 1995; Hernàndez-Enrile, 1991), active during Late Variscan times (Doblas et al., 1994). García-Lobón et al. (2014) present the acquisition processing and interpretation of coincident potential field data (gravity and magnetics) along the ALCUDIA transect. The tectonic evolution and description of the deformation phases of the CIZ can be found in Martínez-Poyatos et al. (2012) and references therein. The ALCUDIA deep seismic reflection transect, runs perpendicular to the geologic structures, imaging the lithospheric section of a large portion of the Central Iberian Zone (CIZ) and its southern limit, the Central Unit (CU).

3. Acquisition and new processing approach

The ALCUDIA deep seismic profile was designed to be a high quality LITHOPROBE style normal incidence deep seismic reflection transect. The profile was perpendicular to the main surface geologic features. It was acquired by an academic crew in 56 days during spring 2007 using Vibroseis sources and a SERCEL 388 seismic acquisition instrument, with a capability of recording up to 400 channels. Besides local relief due to lithological contrasts, the long term undulating topography along the profile varies from about 500 m in the southern/central part to 800 m in the northern part (Fig. 1e). The transect can be considered a northern extension of the IBERSEIS normal incidence transect (Simancas et al., 2003), therefore, very similar acquisition parameters (Table 1) were used. In order to better image the shallow sub-surface the source was activated every 70 m and an asymmetric split spread with 35 m station spacing was used. Four Vibroseis trucks were used to generate 20 s long nonlinear sweeps within frequency range of 8–80 Hz. In total, 3622 VPs were generated. Each VP consisted in six nonlinear sweeps. The configuration resulted into a common midpoint (CDP) spacing of 17.5 m with a nominal CDP fold of 60. The transect followed mostly unpaved roads whenever possible; however it went through few villages. In the inhabited areas sources could not be activated, therefore, to avoid data gaps villages were under shoot. The VP spacing a few kms before and after the villages the source spacing was reduce to 35 m and the spread length was increased. This help to avoid large fold variation beneath inhabited areas.

The raw seismic data show sufficient high signal to noise ratio and occasionally relatively high amplitude reflections can be observed at

Please cite this article as: Ehsan, S.A., et al., Crustal deformation styles along the reprocessed deep seismic reflection transect of the Central Iberian Zone (Iberian Peninsula), Tectonophysics (2014), http://dx.doi.org/10.1016/j.tecto.2014.02.014

Table 1
Acquisition parameters for the ALCUDIA seismic profile (modified after Martínez-Poyatos et al., 2012).

Profile	ALCUDIA
Type of survey	2D crooked line
Recording system	SERCEL 388
Nominal spread	Asymmetrical split spread
Nominal fold	60
Source type	Vibroseis
No. of Vibroseis trucks	4 (+1 spare) 22 TM
No. of Sweeps per VP	6
Sweep length	20 s
Sweep type	Nonlinear
Sweep frequencies	8–80 Hz
Nominal VP interval	70 m
Total No. of VP	3622
Geophones	Group of 12, 10 Hz
No. of active channels	240
Receiver interval	35 m
Field low cut filter	Out
Recording length	40 s (20 s after correlation)
Sampling rate	2 ms
Maximum offset	8900 m
Total length	230 km
Date acquired	01/05–25/06, 2007

shallow and deep levels. Martínez-Poyatos et al. (2012) presented the first stacked images of the data and were able to place constraints on a large scale crustal structural model. The current work has devoted a large effort in enhancing the shallow reflectivity features in order to be able to directly correlate the interpreted structures in the seismic cross section with the surface outcrops. Furthermore, special attention has been placed in the fabric of the deep reflectivity to obtain clear geometries and estimates of their position in depth. In summary, the new processing strategies (Table 2) have pursued: prestack signal enhancement; stacking velocity models for normal moveout (NMO) corrections; detailed statics; DMO; migration; and depth conversion. Some of this has proven beneficial; others have not been that effective (for example DMO, which is discussed later in the text). The interpretation by Martínez-Poyatos et al. (2012) suggested a relatively high degree of structural complexity. There are for example a number of high dip structures, even subvertical features. This will need special attention, designing the static correction, NMO velocity model, migration, and depth conversion.

Table 2
The principal processing parameters.

Parameters	
1) Read SEG-Y data	20 s
2) Resample	4 ms
3) Apply geometry	Crooked line
4) First arrival picking	Automatic & manual
5) Trace edits	Manual
6) Refraction statics	Datum 630 m, single layer model, bedrock 5000 m/s, overburden 2900 m/s
7) Band pass filtering	Time-variant filtering 0–2500 ms: 18–30–70–80 Hz 2600–5000 ms: 15–25–60–70 Hz 5100–8000 ms: 10–20–50–60 Hz 8100–12,000 ms: 10–15–45–50 Hz 2000–20,000 ms: 10–17–40–50 Hz
8) Surface wave attenuation	FK Filter 9 ms/trace
9) Wiener deconvolution	Filter length 150 ms, gap length 16 ms
10) Airwave filter	330 m/s
11) SD compensation	Forward
12) Velocity analysis	Iterative
13) NMO corrections	40% stretch mute
14) DMO corrections	60% stretch factor
15) Residual statics	Twice & iterative
16) CMP Stacking	Unity
17) FX-deconvolution	100 ms 50 traces
18) Migration	Stolt 5000 m/s (Poststack) Kirchhoff 5500 m/s (Prestack)
19) Depth conversion	0–5000, 10,000–6200, 10,000–6200, 20,000–8000 ms–m/s

The entire seismic section is characterized by very limited sedimentary cover. Therefore, it can be considered that the data was acquired in relatively high velocity crystalline crust. A large percentage of the surface outcrop along the line composed of quartzite, slate and granite (Fig. 1c). Considerations that are effective in this environment where carefully considered (e.g., Cheraghi et al., 2011; Heinonen et al., 2013; Juhlin et al., 2010; Schmelzbach et al., 2007). A substantial amount of effort was spent on processing scheme to preserve relative true amplitudes. The useful frequency content determined from filter panels was considered to be of 10–50 Hz. A smooth crooked CDP line with a CDP spacing of 17.5 m was used for stacking. The selected CDP line was close to the actual receiver source positions along the profile whereas the orientation of the CDP bins are defined in a way to minimize the loss of midpoint traces. The trace editing was performed to remove noisy traces and a spherical divergence correction was applied on the data to compensate for the loss of energy due to attenuation and scattering (Robinson and Coruh, 1988). The reflections in the raw shot gather (Fig. 2a) are masked by random noise and coherent events (i.e., shear wave energy and ground roll, and reverberations). The amplitude of these events was attenuated by time-variant band pass filter and predictive Wiener deconvolution. The selected parameters (time and frequency windows) for the time-variant band pass filter (i.e., decreasing frequency band with increasing time) helped to enhance the deeper reflections. On the recorded shot gathers, the surface wave energy especially at shallow travel times was attenuated by frequency–wavenumber filtering (F–K). The variation in elevation and thickness of the overburden and the significant velocity contrast between the overburden and the bedrock produce large travel time variations (Robinson and Coruh, 1988; Yilmaz, 1989). The first arrivals (i.e., direct and refracted energy) were picked automatically followed by rigorous manual inspection for a good estimate of refraction statics to correct for the time delays. For refraction static corrections, a single layer model consisting of an overburden with the velocity set to 2900 m/s and crystalline bedrock with the velocity set to 5000 m/s was chosen. Our final static model is reasonably smooth and consistent and shows a RMS-misfit target of 7 ms (Fig. 3a). The processed shot record (Fig. 2b) reveals a series of dipping reflections which are better imaged after the application of the prestack processing flow. The amplitude spectra after prestack signal enhancements benefited from the increase in the energy of the high frequencies which indicates that a moderate increase in the vertical resolution was achieved by the processing flow (Fig. 2c and d).

The raw shot records were sorted into CDP domain and NMO corrected. Careful velocity analysis was done prior to the stacking of data. Surface geology reveals numerous steeply dipping structures (for example in the southern end of the line) and high angle folds, south of the Almadén Syncline (Fig. 1c and d). High stacking velocities were required to image these dipping structures. To calculate the optimum stacking velocities constant velocity stacks were carried out for a velocity range from 5000 m/s to 13,000 m/s with an increment of 500 m/s. Since stacking velocities are dip dependent, dipping reflections stacked coherently at higher stacking velocities while sub-horizontal reflections stacked coherently at lower stacking velocities. The choice of the stacking velocity function has a significant influence on the image quality and is also important for the proper estimation of residual statics (Malehmir and Juhlin, 2010). The residual static corrections were estimated on the NMO corrected gathers and improved the lateral continuity of the events within the section. In theory the DMO process aims to resolve conflicting dips, thus stacking velocities become independent of dip, and helps to improve the velocity function (Deregowski, 1986: Yilmaz, 2001). Nevertheless, the application of the DMO on this dataset did not improve the resolution and many reflections became weaker and less continuous. The failure of the DMO is probably due to the

Please cite this article as: Ehsan, S.A., et al., Crustal deformation styles along the reprocessed deep seismic reflection transect of the Central Iberian Zone (Iberian Peninsula), Tectonophysics (2014), http://dx.doi.org/10.1016/j.tecto.2014.02.014

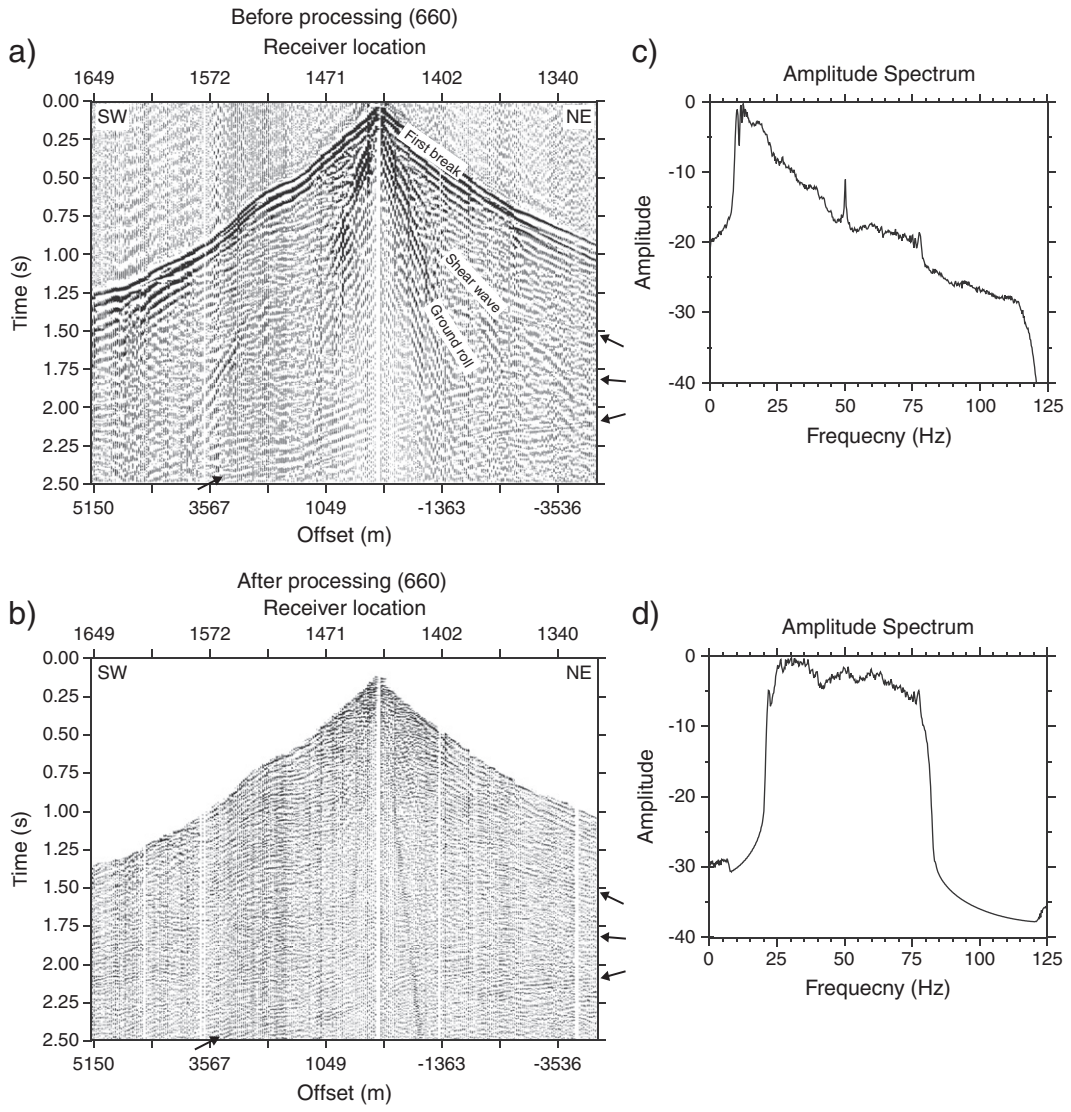

Fig. 2. An example of raw shot gather from ALCUDIA deep seismic reflection profile (a) before processing and, (b) after processing; source point 660. The source generated noise and random noise were reduced by the processing sequence applied. After the processing an increase of signal to noise ratio is observed. These enhanced reflections are marked by black arrows. The frequency content was also modified by the processing flow, resulting in a better balanced response. The amplitude spectra before and after processing is displayed in (c) and (d), respectively.

crookedness of the profile (Deregowski, 1986; Juhlin et al., 2010). The final stack section (Fig. 3d) shows moderately to steeply dipping and subhorizontal reflections at both shallow and deep levels. For display purposes a coherency filtering (FX-deconvolution) was applied after stacking to attenuate the random noise.

The stack section reveals a series of vertical strips (Fig. 3d) where signal to noise ratio is low. These vertical bands are roughly coincident with the thickest syncline structures (which are cored by Ordovician to Devonian alternating slates and quartzites) observed at the surface (Figs. 3d and 4b). The poorly imaged bands are related to the limitation of seismic reflection method over steeply dipping limbs of folded structures (e.g., Heinonen et al., 2012; White et al., 2000). Note the correlation of the relatively low signal to noise ratio beneath the Guadalmez syncline, the Almadén syncline, the Herrera del Duque syncline and the Navalucillos syncline. The data quality beneath the Guadarranque syncline is also characterized by low signal to noise ratio but is not as low as observed beneath the other synclines. On the contrary, these synclines show enhanced reflectivity in the range of c. 0–1 s, (0 to 3 km depth). This could be attributed to contrasting impedance in the Ordovician to Devonian successions and/or structure shallowing with depth. The stack was then migrated so that the subsurface structure would be closer to the real geometry and the reflectors would be placed to their true subsurface position and the corresponding dips should be close to true dip. This is correct in laterally homogeneous velocity model. Note that the line was acquired on crystalline terrain and the surface outcrop is indicative of a relatively high degree of heterogeneity in the subsurface. Nevertheless, in order to get a reliable representation of the subsurface, a series of tests, with different velocity fields, on the available poststack time migration algorithms such as Kirchhoff, finite-difference, phase-shift, and Stolt were performed. Stolt and phase-shift migration approaches provided qualitatively better results for a constant velocity of 5000 m/s. Initially, the NMO velocity model was used for depth conversion, but the relatively large degree of lateral velocity variability did not produce a better image. For the depth conversion, an average velocity of 6200 m/s for the crust and 8000 m/s for the reflections beneath the Moho were used (Fig. 4a).

4. A cross section across the CIZ from the ALCUDIA deep seismic reflection image

The ALCUDIA normal incidence deep seismic profile (Figs. 3d and 4a) reveals highly reflective crust down to depths of c. 31 km. The

Please cite this article as: Ehsan, S.A., et al., Crustal deformation styles along the reprocessed deep seismic reflection transect of the Central Iberian Zone (Iberian Peninsula), Tectonophysics (2014), http://dx.doi.org/10.1016/j.tecto.2014.02.014

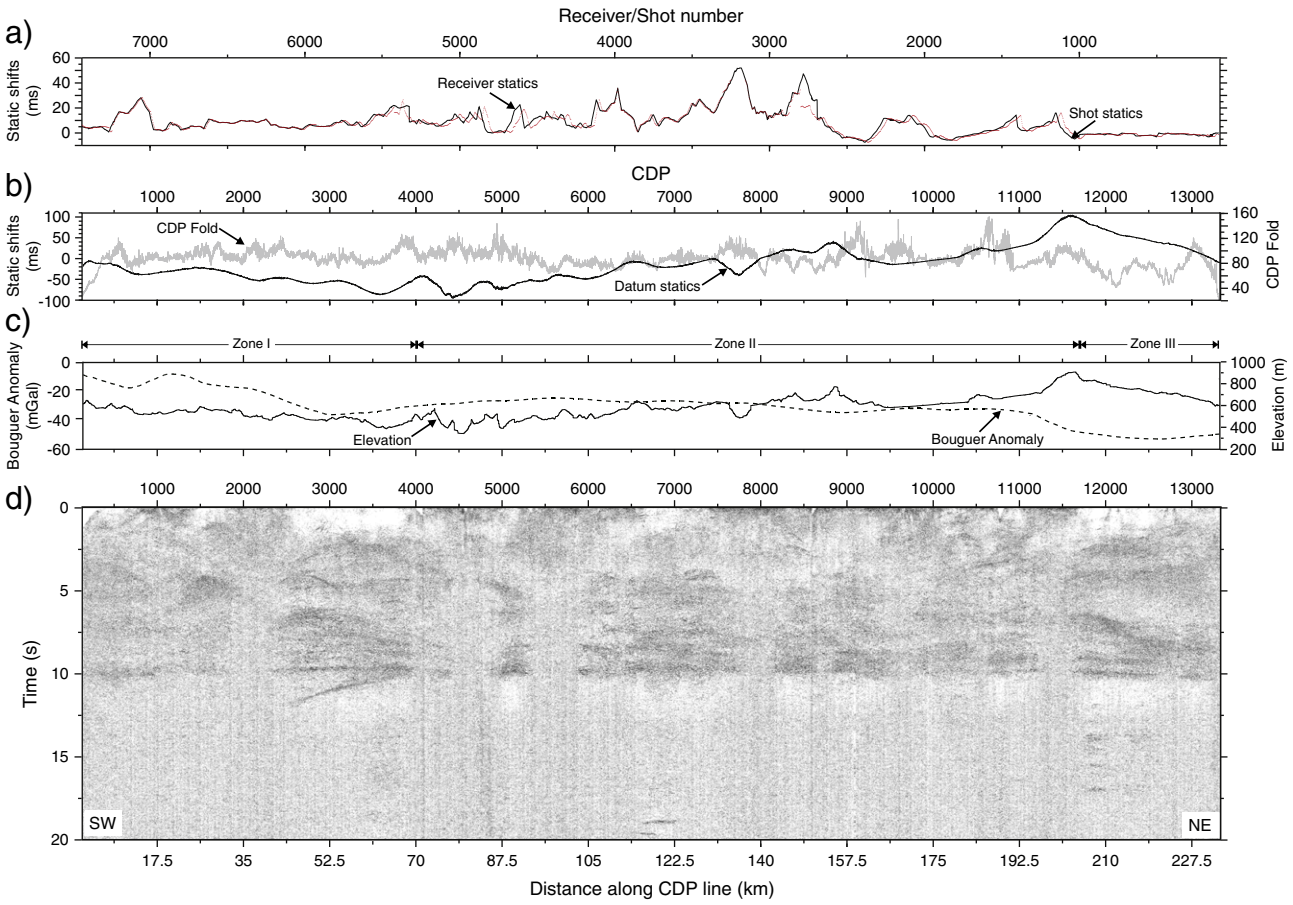

Fig. 3. (a) Receiver and source statics, (b) CDP fold coverage (relatively high fold over 60) and datum statics and, (c) Bouguer gravity anomaly along the ALCUDIA deep seismic reflection profile and the topography of the transect. (d) The ALCUDIA deep seismic reflection profile, unmigrated stack section.

high quality data features complex geological structures and numerous reflections with various dips and lengths. The ALCUDIA transect was acquired perpendicular to the strike of main geological structures, therefore, most of the events can be interpreted as reflections located within-the-plane of profile. A small number of events have been identified as related to over-migration artifacts. These are located at shallow levels and occasionally appear within the lower crust (Fig. 4a). They are, most probably due to discrepancies in the velocity model used for the migration. The reflectivity in the upper part shows good correlation with the surface geology, and this knowledge guided the interpretation of most of the seismic events and fabrics. The new interpretation complements the relatively large scale model developed in Martínez-Poyatos et al. (2012). The seismic cross-section is analysed from south to north. The upper crust of the CIZ can be considered in average c. 13 km thick. Taking the observations from the surface outcrop jointly with the seismic image the transect can be roughly divided (in general terms), in three parts with distinctive characteristics depending on the seismic reflection fabric (Fig. 4b and c). From south to north, the section can be divided in; Zones I, II and, III.

4.1. Zone I

This is a heterogeneously deformed zone, which can be determined from the southern end of the line up to CDP 4000, which at surface would correspond to the southern flank of the Guadalmez syncline. This portion includes a major suture zone, (the Tomar–Badajoz–Cordoba shear zone where the most representative unit is the CU) and highly deformed bounding areas (e.g., Espiel Thrust Sheet) (Fig. 1c and d). This zone would represent c. 70 km wide area of deformation (mostly transpressive deformation); it also features a series of plutonic intrusions, the most representative of which is the Pedroches Batholith.

4.2. Zone II

This part would represent a less deformed zone which would have accommodated a small fraction of the compressive deformation. The accommodation would have taken place in the development of a series of synclinal and anticlinal geologic structures. There are five well marked synclines (Guadalmez syncline, Almadén syncline, Herrera del Duque syncline, Guadarranque syncline and Navalucillos syncline) in between them there are four anticlines (Alcudia anticline, Esteras anticline, Navalpino anticline, and Valdelacasa anticline) (Figs. 1c and 4c). At relatively shallow layers this Zone II mostly consists of a deformed layer cake lithology (mostly alternating slate and quartzite) (Fig. 1c and d). These folds can be cored by blind thrust of relatively small dimensions (a few km). This blind thrusting is suggested by the seismic fabric of the upper crust.

4.3. Zone III

This part would correspond from CDP 11,700 up to the northern end of the seismic transect and in outcrop this includes the Mora Pluton and the southern part of the Toledo Anatectic Complex, with the tectonically relevant Toledo Fault (TF). This last part is apparently the least affected by compression at the surface. The geologic evidence, surface outcrops and the structure suggested by the seismic reflection image indicate that the area has been affected by a major extensive tectonic event responsible for the, relatively, low angle fault systems. The mid-lower crust with an estimated thickness of c. 17 km features relatively high

Please cite this article as: Ehsan, S.A., et al., Crustal deformation styles along the reprocessed deep seismic reflection transect of the Central Iberian Zone (Iberian Peninsula), Tectonophysics (2014), http://dx.doi.org/10.1016/j.tecto.2014.02.014

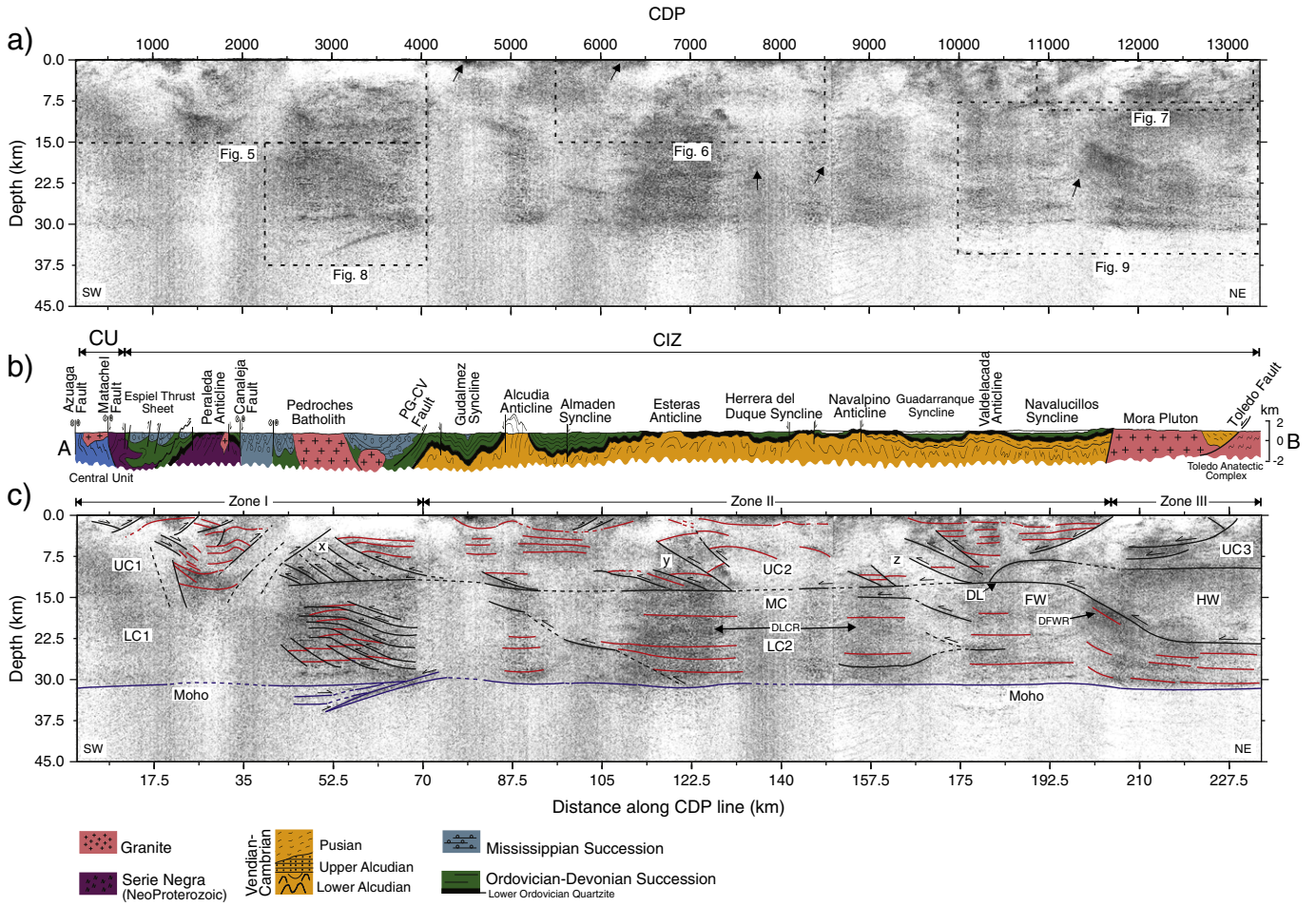

Fig. 4. (a) Poststack migrated (15 s) and depth converted section. The locations of the expanded areas which are discussed in the text are marked in the image. These are presented in Figs. 5, 6, 7, 8 and 9. (b) The geological cross section along the ALCUDIA profile. (c) The suggested interpretation of the migrated and depth converted ALCUDIA profile. The black thick lines have been interpreted as faults and/or major shear zones; the red lines are indicative of the trends of the most prominent reflectivity fabric. The crust–mantle transition is highlighted by a blue line. Abbreviations: UC, Upper crust; MC, Middle crust; LC, Lower crust; DL, Decollement level; HW, Hanging wall; FW, Footwall; DLCR, Dense lower crustal reflectivity; DFWR, Dense footwall reflectivity; x, y, z, imbricate thrust systems (see text for further interpretation). The overall extension of the Zones (I, II, and III) discussed in the text is also marked.

amplitude reflectivity fabric which suggests a laminated lower crust beneath the CIZ (Fig. 4a and c).

By contrast, the mid-lower crust of the southernmost end of the transect under the CU features a diffused reflectivity pattern and lacks localized events which would correspond to the OMZ crust. The Moho discontinuity at an approximate depth of 31 km is the most prominent feature of the image, and it changes character along the profile most probably revealing differences in its nature (Carbonell et al., 2013).

4.4. Upper crust of the CIZ

The seismic images reveal patches of reflectivity which feature characteristic trends (dip attitude, amplitude, and lateral continuity) which appear to complement the surface observations. For example the relatively high angle dips of the events in the southern and northern most parts of the seismic images suggest a complex degree of faulting and/or folding (Fig. 4a and c). The southern end of the transect images the suture zone that separates the OMZ from the CIZ where the CU has been described (Azor et al., 1994; Burg et al., 1981; Simancas et al., 2001). This section overlaps with the IBERSEIS transect (Simancas et al., 2003, 2013) which is located, approximately, 70 km to the NW (Fig. 1b). The image of the suture reveals geometry with similar structures as interpreted in the IBERSEIS profile. The northeast dipping reflections from CDPs 1000 to 1500 are observed at c. 3 to 9 km depth (Figs. 4c and 5). These reflections probably represent the depth extension of the highly sheared CU, cut by the Espiel thrust at c. 2.5 km depth. The Azuaga Fault (AF), subvertical at surface, marks the southernmost limit of the transect (Fig. 1c) and mainly due to lack/reduced fold coverage the fault is not seen in the stack section. However, a steep north dipping event that intersects the first arrivals can be identified in shot gathers from 3590 to 3622 (Fig. 5c). This corresponds to the station located on top of the surface outcrop of the Azuaga Fault zone. A series of south dipping events can be identified at the location of CDPs 850 to 1250, c. 0 to 3 km depth. These events appear to correlate with surface outcropping south dipping faults which correspond to the northeast vergent Espiel thrust sheet. Note also that the seismic fabric denotes that the crust has been strongly folded and sheared revealing that this part concentrates relatively large amount of deformation (Figs. 4c and 5). For example, within a relatively short horizontal distance the reflectivity patterns change dip. This contrasts with the rest of the profile, where the folding is less intense and the reflected events feature smaller dips. Within CDPs 100 to 4000 (Zone 1) (Fig. 5), the crust is characterized by a relatively high degree of complex structures denoting intense strain/deformation. The deformation due to the collision is most probably localized near the main suture zone (the CU) and decreases towards the north (increasing CDP numbers). The shallow northeast and southwest dipping reflections within CDPs 1000 to 1750 can be associated to the Peraleda anticline (Figs. 4c and 5). This structure, the Peraleda anticline is cut by a thrust fault that projects to the surface approximately at CDP 1490. The reflectivity

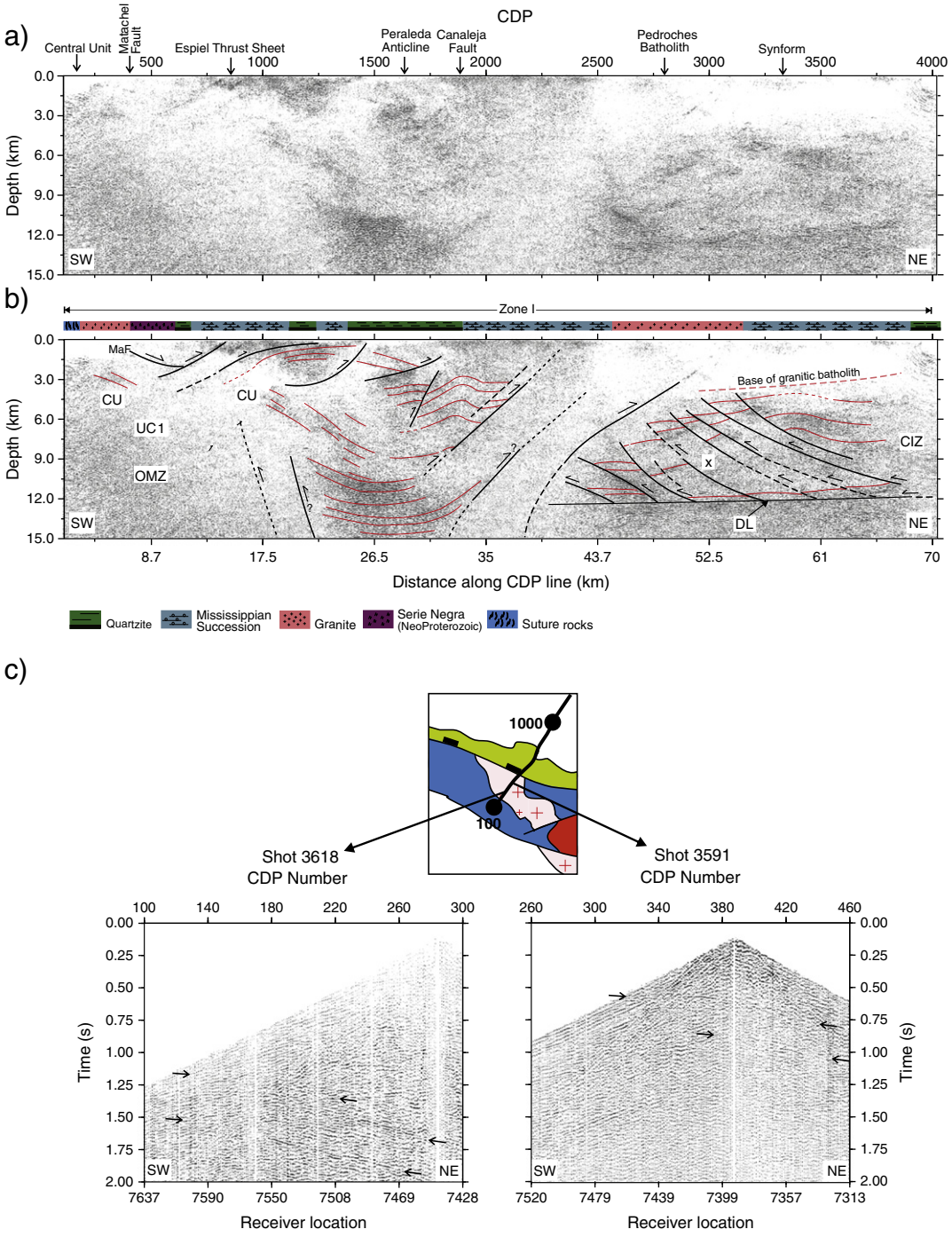

Fig. 5. (a) Uninterpreted and, (b) interpreted migrated depth sections of the upper crust along the southern portion (Zone I) of the ALCUDIA deep seismic reflection profile. The images reveal a good correlation between the reflections in the shallow crust and the surface geology. The high angle oblique faults represent more intense deformation close to the deformational front. (c) The selected shot gathers (3618, 3591) after processing. These shot records show a band of north dipping reflections highlighted with black arrows. This band of reflections correlates with the southern limit of the Azuaga Fault. Abbreviations: CIZ, Central Iberian Zone; CU, Central Unit; OMZ, Ossa–Morena Zone; MaF, Matachel Fault; DL, Decollement level; x, imbricate thrust system (see text for further interpretation).

fabric decreases in amplitude just beneath the entire extension of the Peraleda Anticline. This lack of reflectivity under the core of the anticline suggests that it might be due to the presence of a southern extension of a small granitic pluton (the Valsequello stock) at the surface. The amplitude of the reflectivity is recovered between the Canaleja Fault and the southern limit of the Pedroches Batholith a major Late Variscan Igneous plutonic complex. The Pedroches Batholith lacks a characteristic reflectivity fabric which is typical of undeformed plutonic bodies. There is a lack of a clear reflection fabric until 4.5 km depth. This most probably denotes the base of this intrusive body at c. 4.5 km depth, in accordance with the interpretation by Aranguren et al. (1997) as a thin laccolith intrusion. The reflectivity gap has an extension of approximately 27 km in length, although the pluton only outcrops for about 14 km, which indicates that the Pedroches Batholith continues northwards below the Mississippian sediments (Fig. 5b).

The amplitude level of the near surface reflectivity fabric is nearly continuous from CDP 4000 until CDP 11,700 (Zone II). At this location the southern limit of the Mora Pluton has been mapped at the surface. From CDP 4000 (the surface location of the PG–CV Fault), until CDP 11,700, approximately the reflection fabric suggests an undulating

Please cite this article as: Ehsan, S.A., et al., Crustal deformation styles along the reprocessed deep seismic reflection transect of the Central Iberian Zone (Iberian Peninsula), Tectonophysics (2014), http://dx.doi.org/10.1016/j.tecto.2014.02.014

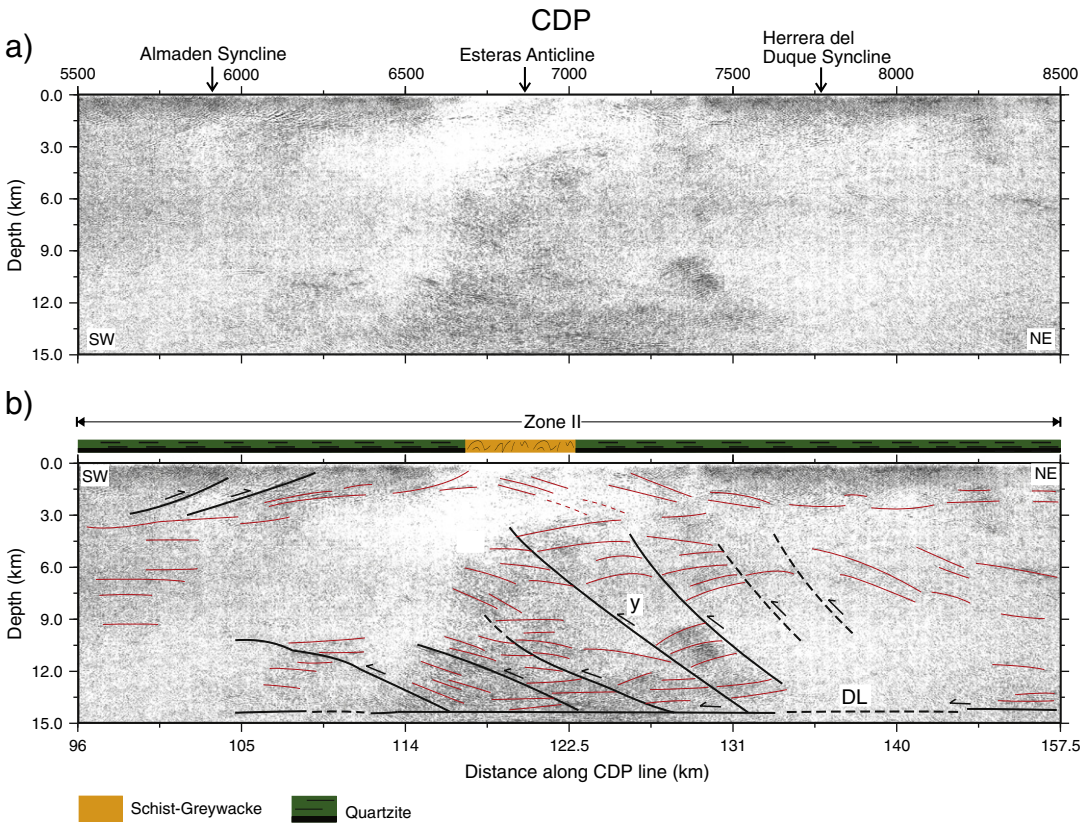

Fig. 6. (a) Uninterpreted and, (b) interpreted migrated depth sections of the upper crust along the central portion (Zone II) of the ALCUDIA deep seismic reflection profile. The reflections in the upper crust show a good correlation with surface geology. An imbricate thrust system (y) is defined that soles down in a basal decollement at approximately, mid crustal level (see text for further interpretation).

series of surface structures with enhanced reflectivity in the synclines (Ordovician to Devonian rocks) (Figs. 4c and 6). Between this CDP range (4000 to 11,700) there are two localized spots where the reflectivity weakens: one in an area centred, approximately at CDP 5000 and a second centred, approximately at CDP 7000. These coincide with the Alcudia and Esteras anticlines, where the Ordovician to Devonian succession is missing and the Neoproterozoic to Cambrian (Schist–Greywacke Complex) succession outcrops in anticlinal structures. Below the surface fold-train, reverse faulting (blind thrusts) probably accompanied the folding in the upper crust (c. 3 to 12 km depth) (Fig. 6). The deep reflectivity of central part of the upper crust from about CDPs 2500 to 10,500 (Figs. 4c, 5 and 6) shows an imbricate character of folds and reverse faults. Three sets of southwest verging imbricate thrust systems (x, y, and z in Fig. 4c) are recognized along the southern and central part of the upper crust. The set of north dipping reflective bands, most probably represent a thrust fault system featuring small displacement that merge in the subhorizontal reflective band interpreted as a basal decollement (DL) which separates the upper crust from the mid-lower crust at a depth of c. 13 km.

Towards the northern end of the transect the surface outcrop reveals evidences of extensional faulting, the Toledo Fault (TF) being the major example (Barbero, 1995; Hernàndez-Enrile, 1991). The majority of the observed reflectivity correlates with the surface geology. We interpret a series of southwest dipping reflections which are indicative of, relatively, low angle faults (TF, MF, F1, F2, F3) (Fig. 7). In the seismic image, the Toledo Fault (TF) can be interpreted as a south dipping event which, although weak and diffuse near the surface can follow dipping towards the south from CDP 13,100 till CDP 11,800 (Fig. 7). Another prominent reflection projects to the surface at about CDP 11,600, and it appears to correlate with the Mora Fault (MF). The reflectivity of the TF and MF decreases at the surface possibly due to the contact with granitic bodies and soles down at c. 6 km. Reflections F1 and F2 do not extend to the surface whereas F3 merges with the TF. A semi-transparent unit (Mora pluton) is imaged from CDPs 11,600 to 12,600 that extend to depths of about 3 km. The Toledo Fault (TF) also acts as the upper limit of the Toledo Anatectic complex. The Mora Pluton, the Toledo Anatectic complex, and the Toledo and Mora Faults (south dipping fault system) define the geometry of what has been labelled as Zone III (Figs. 4c and 7).

4.5. Middle-lower crust

From southwest to northeast comparing the seismic fabric that characterizes the mid-lower crust of the defined three zones it is observed that in the stack section Zone I features a relatively large population of arcuate reflection segments denoting or suggesting boudinage structures within the mid-lower crust. These suggested lens shape features turn to be horizontally stretched from CDP 4000 onwards, just after the wedge feature that is imaged beneath the Moho (Figs. 3d and 4a). There is also a transition in the vertical direction of the shape of these boudins (Fig. 8). The seismic image reveals a complicated mid-lower crustal structure, which is most probably a result of inter-network of shear zones which result in a relatively large scale boudinage fabric, boudins with a horizontal length of 500 CDPs, (about 7 to 9 km). Another feature which is relevant to point out is a dipping band of weak or lacking seismic reflectivity which starts at the lower crust beneath CDP 1500 and extends to the surface at CDP 2500 very close to the southern border of the Pedroches Batholith. This suggests possible association with the batholith. This zone of weak reflectivity could be interpreted as channel/pathway which would feed the batholith with the necessary granitic magmas. At deeper levels (c. 30 km) and between CDPs 2800 and 3900, a singular wedge structure is imaged, which involves the Moho discontinuity (Figs. 4a, c, and 8). The complex wedge reveals about 18 km of the lower crust featuring relatively high amplitude

Please cite this article as: Ehsan, S.A., et al., Crustal deformation styles along the reprocessed deep seismic reflection transect of the Central Iberian Zone (Iberian Peninsula), Tectonophysics (2014), http://dx.doi.org/10.1016/j.tecto.2014.02.014

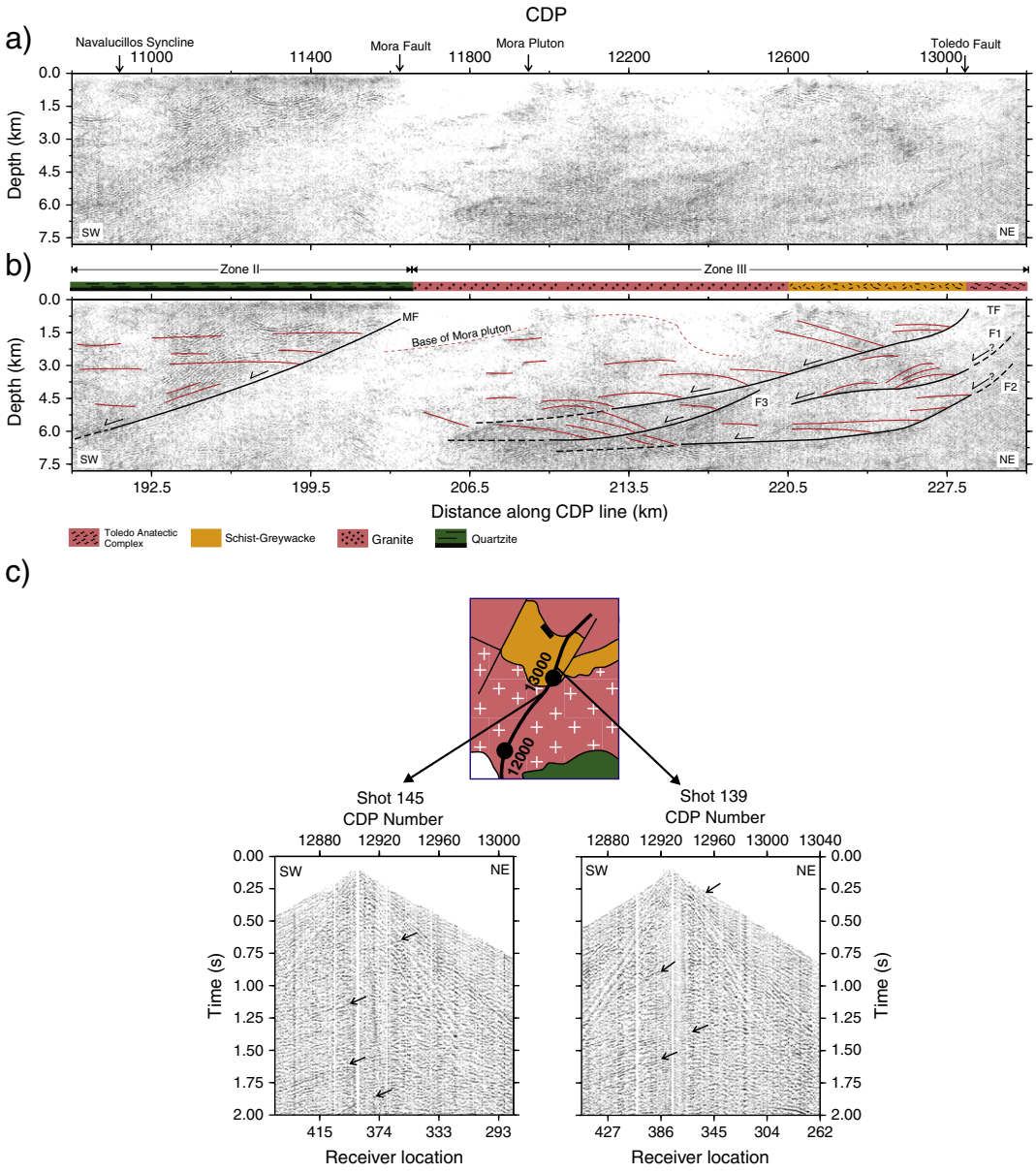

Fig. 7. (a) Uninterpreted and, (b) interpreted migrated depth sections of the upper crust along the northern portion (Zones II and III) of the ALCUDIA deep seismic reflection profile features a complex series of low angle normal faults (TF, MF, F1, F2 and F3). (c) Two processed shots gathers from the northern end of the ALCUDIA transect show a band of south dipping reflections which project to the surface. Abbreviations: TF, Toledo Fault; MF, Mora Fault (see text for further interpretation).

and laterally continuous events which are arcuate at the top (c. 20 to 25 km depth). Beneath the dome like feature there is a marked reflectivity fabric that extends down to the interpreted base of the crust. A possible explanation for this wedge like feature is that it can correspond to the deep representation of the surface identified major suture zone of the CU (Fig. 8). North of the wedge structure and within Zone II, the crustal structure is characterized by a relatively horizontal reflectivity fabric which defines relatively long/stretched boudins (on the order of 1500 to 2000 CDPs in width which corresponds to, 26 to 43 km) about a factor of 4 times wider than the boudins identified in Zone I (Figs. 3d and 4a). The vertical thickness of these boudins is about 1.5 km (which corresponds to, approximately 0.5 of the boudins' thickness identified in Zone I). At this respect, the northern end of the IBERSEIS transect also imaged boudinage features with similar dimensions (Carbonell et al., 2004; Simancas et al., 2003), these were located in the lower crust just north of the outcrop of the CU. The seismic events simulate slices of crustal material (boudins) which have been stacked one on top of the other, along highly reflective shear zones. The structure could be interpreted as the result of a transpressive suture zone where the deformation has been distributed and a large part of the deformation has been accommodated by a flower structure about 52 km of which are imaged and mapped by the ALCUDIA deep seismic reflection image. Note that the IBERSEIS normal incidence transect (Carbonell et al., 2004; Simancas et al., 2003) identified a mid crustal magmatic intrusion which was labelled Iberian Reflective Body (IRB). The current transect corresponds to the northern extension of the IBERSEIS, and such a mid crustal high amplitude reflectivity structure is not identified. On the other hand, the prominent and complex boudinage fabric is limited by a weak reflectivity feature that appears to connect to the surface just beneath the Pedroches Granitic pluton. This could correspond to a channel used by the granitic magmas that ended up at the surface as the Pedroches Batholith. The seismic reflection fabrics imaged beneath Zone I, the bivergent system of faults within the upper crust and the south vergent pathway characterized by the lack of reflectivity (Figs. 4c and 5) and the complex structure at the Moho beneath CDPs 2800 to 3900 can be integrated into a crustal scale deformed flower structure. Crustal scale transpressive shear zones and/or large scale strike-

Please cite this article as: Ehsan, S.A., et al., Crustal deformation styles along the reprocessed deep seismic reflection transect of the Central Iberian Zone (Iberian Peninsula), Tectonophysics (2014), http://dx.doi.org/10.1016/j.tecto.2014.02.014

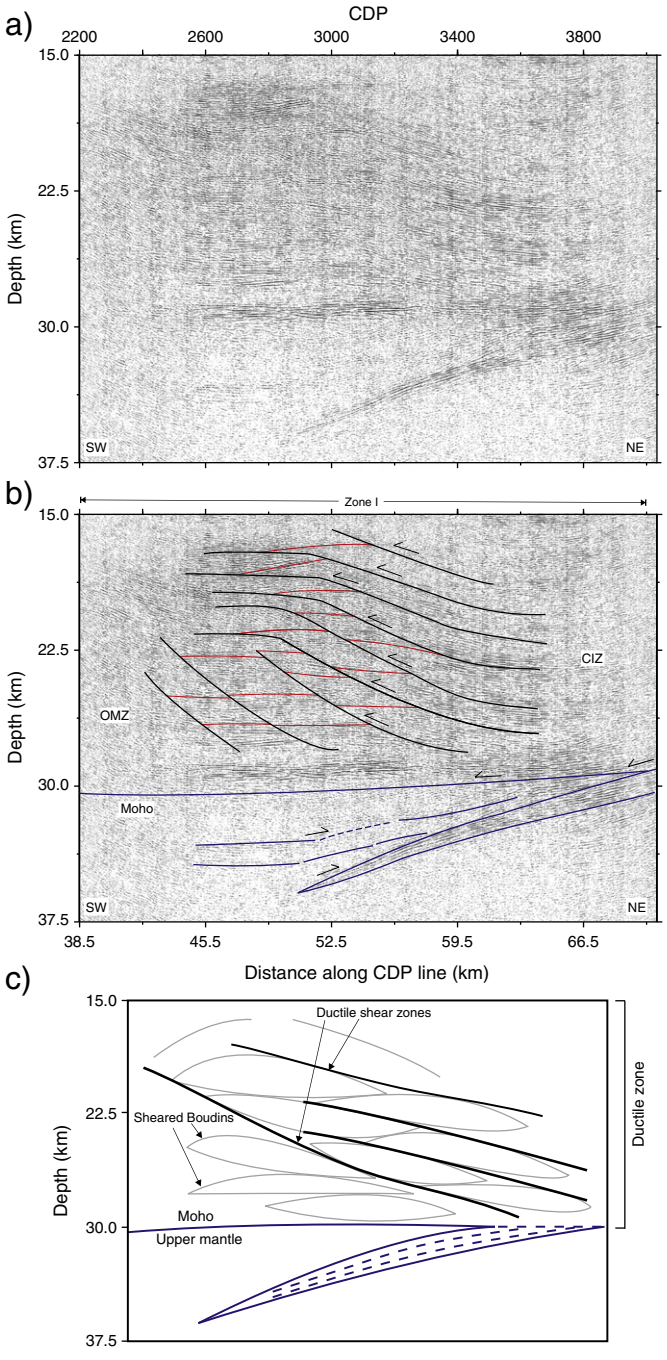

Fig. 8. (a) Uninterpreted and, (b) interpreted migrated depth sections of the mid-lower crust along the southern portion (Zone I) of the ALCUDIA deep seismic reflection profile. The mid-lower crust shows a large population of dense reflections, oblique to horizontal, suggesting boudins (lenses). The boudins are limited by marked shear zones which reveal a laminated reflectivity character. At the Moho level a tectonic wedge has been interpreted, it involves the lower crust and the upper mantle. (c) 2D schematic diagram of the mid-lower crust ductile zone; the lenses (boudins) slide along the inter-network of shear zones.

slip fault zones are able to involve the upper mantle which result in the generation of melts (Pirajno, 2010). The Pedroches pluton can be the surface expression of this crustal scale and probably deformed flower structure.

The change of seismic fabric between the shallow crust, above 12–14 km, and the seismic fabrics at deeper crustal levels evidence a major change in how the strain is accommodated (Simancas et al., 2013). At shallower levels, in Zone II folding accounts for the deformation (Figs. 4c and 6). These folds, below the surface, are probably cored by blind thrusts (Fig. 6) which accommodate the transpressive shortening that accumulated during the collision and was not accounted for in the development of the flower structure in Zone I. Therefore, the folds near the suture zone (the Badajoz–Cordoba shear zone) feature nearly subvertical limbs. Towards the north the folds are less pronounced indicating a decrease in the amount of deformation in the northeastern direction. It is very important to keep in mind that shortening was also accommodated by deformation and material movement in and out of the plane of the seismic image. The mid-lower crust accommodated the deformation within, by a mechanics that generated nearly horizontal seismic reflection fabric. Note that the change in the deformation style corresponds to a relatively sharp discontinuity at c. 12–14 km depth, which most probably corresponds to the ductile–brittle transition. This feature (the brittle to ductile transition) was also evident within the IBERSEIS deep seismic reflection image (Carbonell et al., 2004; Simancas et al., 2003).

The Zone II (CDPs 4000 to 11,700) features a relatively marked vertical change in the seismic signature which is located at a depth of c. 12–14 km. Above this depth the reflectivity is somewhat diffuse with some events which are mostly dipping either to the north or to the south (see for example events labelled y and z in Figs. 4c and 6). Beneath this depth, the reflectivity fabric denotes a relatively large number of laterally continuous packets of events which are mostly horizontal and/or slightly curved (downwards) which flatten at the Moho depth. These packets have lengths that can extend to, almost 1000 CDPs, over more than 15 km in length. Zone II at the surface extends till CDP 11,700, at depth; it probably extends up to CDP 10,500. It could be suggested that this location is the southern limit of the extensional fault system where it soles into the brittle to ductile transition. The south dipping feature can be projected to the surface at approximately CDP 13,100 (the TF in Figs. 4c and 7), an extensional fault of Late to post Variscan age. Fig. 7 reveals that the TF is part of a system of, mostly extensional faults. These geometrical relationships suggest that this feature could also be considered as a pathway that would have feed the granitic pluton.

Beneath the MF, the seismic section reveals a subhorizontal to south dipping event from CDPs 11,200 to 10,400 which can be taken as the top limit of the mid-lower crust (Fig. 9). The most prominent feature is a high amplitude c. 0.8 km thick continuous band of reflectivity, located at c. 23 km beneath CDP 13,100. This sequence of reflectivity is subhorizontal up to CDP 12,300 where it rises towards the southwest and reaches CDP 11,000 at c. 15 km. This well-marked feature has been interpreted as a lower crust thrust that enabled extension at surface (the TF and related normal faults) (see Martínez-Poyatos et al., 2012 for further explanation). Thus, the south dipping extensional fault zone in the upper crust and the thrust dipping to the north in the lower crust define Zone III. The hanging wall of the lower crustal thrust is highly deformed and features low amplitude and discontinuous reflectivity. The southwest dipping reflectivity of the hanging wall is truncated by a sequence of thrust faults that merge in the lower crustal thrust (Fig. 9).

The Mohorovicic discontinuity beneath Zone II is a high amplitude band of reflectivity which beneath Zone III splits into a double horizontal band of reflections (Fig. 9). The Moho beneath Zone II can be considered to be about 1.5 to 2.1 km thick. This Moho contrast with the Moho imaged beneath Zone I which is a very thin feature less that 400 m. The lower crust of Zone II is highly reflective and its base, the Moho discontinuity, is located c. 31 km depth. The overall geometry of the Moho is flat with minor undulations and its internal fabric is subhorizontal. The most outstanding feature below the Moho discontinuity is the southwest dipping mantle wedge between CDPs 2800 to 3900 at c. 30 to 36 km (Figs. 4c and 8). Below the Moho, the upper mantle is almost transparent and reflections are limited to deep zones at 18 to 19 s (65 to 70 km depth) over CDPs 6500 to 7000 and 16 to 17 s (45 to 55 km depth) beneath CDPs 11,700 to 12,500 (Fig. 3d). The thickness of the

Please cite this article as: Ehsan, S.A., et al., Crustal deformation styles along the reprocessed deep seismic reflection transect of the Central Iberian Zone (Iberian Peninsula), Tectonophysics (2014), http://dx.doi.org/10.1016/j.tecto.2014.02.014

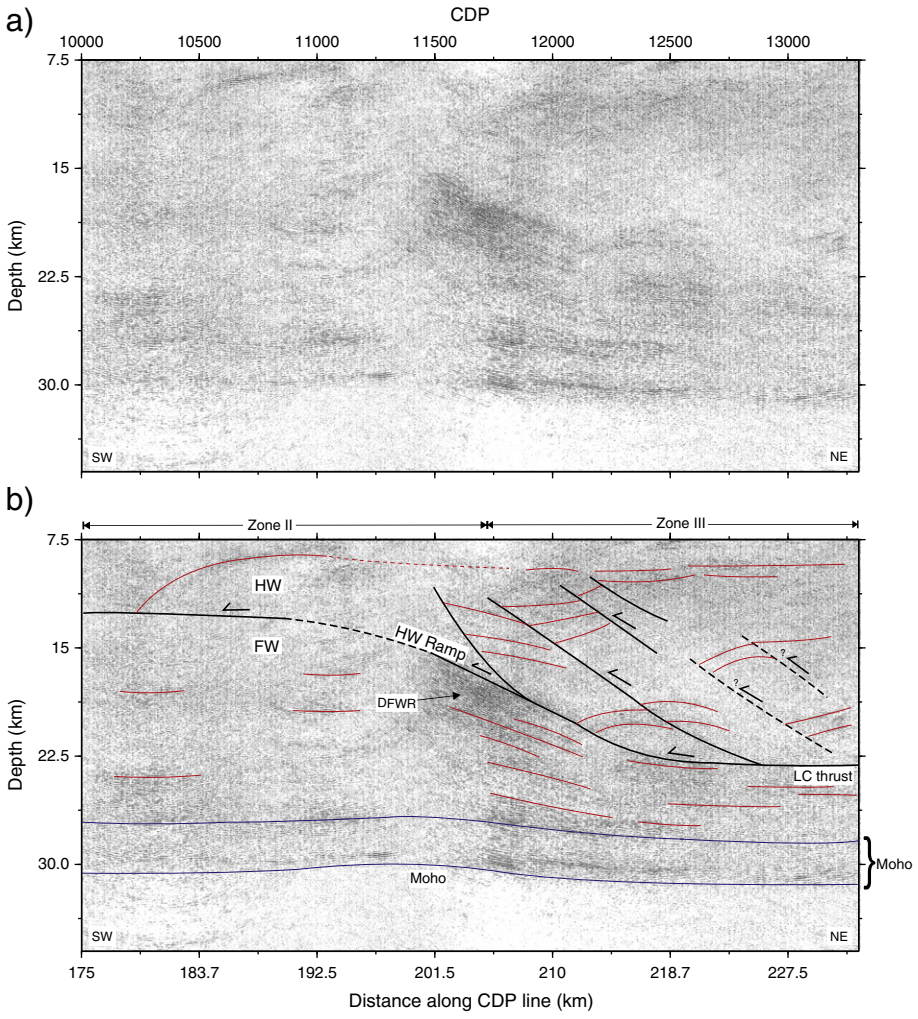

Fig. 9. (a) Uninterpreted and, (b) interpreted migrated depth sections of the mid-lower crust along the northern portion (Zone III) of the ALCUDIA deep seismic reflection profile showing a flat–ramp–flat structure at the mid-lower crustal level. The hanging wall (HW) is highly deformed and less reflective than the footwall (FW). The lower crust is laminated and the Moho discontinuity is split into double bands of horizontal reflectivity (see text for further interpretation).

mid-lower crust in the northern and southern zones is relatively higher than the central zone of the ALCUDIA transect.

5. Discussion

The ALCUDIA profile provides a high resolution and reliable image of the crust and upper mantle down to depths of about 45 km (15 s TWTT; Figs. 3d, 4a, c, 10a, and b). Both, the IBERSEIS and the ALCUDIA seismic profiles demonstrate that the CIZ overthrust the OMZ, resulting in the formation of Devonian recumbent folding and thrusting decoupled from the lower crust in the footwall, and back-folding and back-shearing in the hanging wall (Simancas et al., 2001). The upper crust interpretation of the ALCUDIA profile is based on the surface geological observation, regional geological knowledge and reflectivity patterns (Fig. 10a and b). The normal faults in the upper crust are interpreted on the ALCUDIA profile by their direct correlation with the surface structures. The deep structural framework of the ALCUDIA profile comprises high amplitude, horizontal to subhorizontal, laterally coherent reflectivity and gently to steeply dipping reflections. Large scale strike-slip faults constitute major structures that can extend to lithospheric depths (Zengqian et al., 2003). These structures are able to channel mantle material into the subcontinental lithospheric mantle and/or indirectly provide heat that can induce melting of lithospheric material, resulting in igneous activity, characterized by magmatic products, ranging from mafic–ultramafic to granitic, but all with an alkaline signature (Pirajno, 2010). Furthermore, the fractures zones constitute weak zones (and pathways) which can be reactivated by any other tectonic activity that can affect the area. The CU has been identified at the surface as the most representative unit of the suture/transpressive shear zone, the Tomar–Badajoz–Cordoba. At depth, a singular structure, the wedge, is imaged beneath CDPs 2800 to 3900. This feature is a strong candidate to reflect, or constitute evidence of the collision–suture zone at the Moho depth (Martínez-Poyatos et al., 2012; Simancas et al., 2013). The trend of the major structures identified in the surface geology, and similar crocodile type collisional fabrics identified in the northern end of the IBERSEIS transect seems to support this idea (Carbonell et al., 2004; Simancas et al., 2003). Jointly these two structures, the surface and the deep one can be interpreted as part of a crustal scale deformed flower structure generated during the transpressive, strike-slip tectonics.

In the Almadén Mercury deposit, Silurian to Devonian alkali mafic volcanics appear, the age of the Hg mineralization being centred at 340–360 Ma (Hall et al., 1997; Higueras et al., 2000), with some contributions to the mineralization during the Pennsylvanian, 320 Ma (Hall et al., 1997). Its origin is strongly debated, and there is still some discussion on whether it is associated to hydrothermal activity or to alkali mafic volcanics. Hydrothermal systems, for example in Nevada and New Zealand, are known to report cinnabar and stibnite deposits. These are presumably related to Pliocene to recent volcanism and a change from subduction to transform tectonics (Peabody and Einaudi,

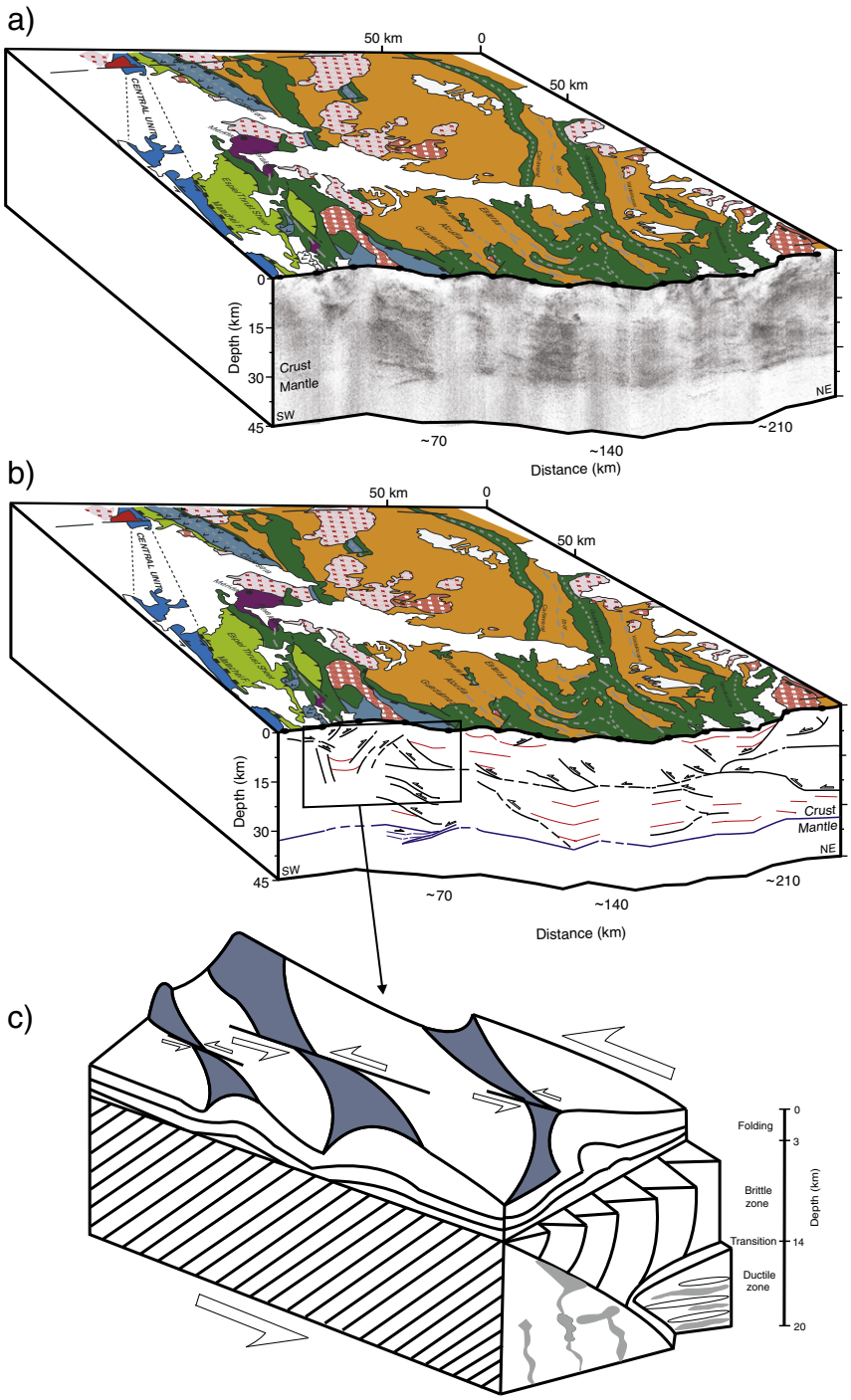

Fig. 10. 3D schematic block of the ALCUDIA transect with the surface geology and the seismic images. (a) Migrated depth section across the Central Iberian Zone (CIZ) and Central Unit (CU) following the crooked line geometry overlain by the geological map for easier correlation with surface geology. (b) The interpretation of the migrated depth section based on regional tectonic knowledge, geological and seismic reflection studies. The resulting undulating topography reflects the accommodation of the fractured elongated blocks in the crystalline basement which were subjected to transcurrent movement due to the transpressive collision during the Variscan. (c) Sketch diagram to resolve the deformation and movement of the blocks within the upper crust, and the sedimentary cover due to the interpreted flower structure. It can be suggested that such a structural setting can provide the necessary pathways and tectonic links for the alkaline basaltic magmas and associated mercury mineralization to be able to rise to the surface.

1992). Other mercury deposits in the Almadén area which are hosted by volcanics seem to indicate a direct relation between mercury mineralization and mantle derived alkaline basaltic volcanics (see for example the Las Cuevas deposit Hernandez, 1984; Ortega, 1986; Ortega and Hernandez, 1992). It is recognized that there is a relatively high contribution related to deep mafic volcanics perhaps of asthenospheric origin (Higueras et al., 2000; among other authors). In the Almadén district at least one feeder pipe of the alkaline basalts and presumably also of the mercury mineralization, is known near the village of Almadenejos but its tectonic control has not been established. Outside the Almadén district, in the Paleozoic of Iberia, this type of volcanism has only been observed in an area in Cantabria (Heinze et al., 1985), where substantial mercury and antimony mineralizations have also known to occur (Maucher, 1976). So the two apparently opposing views are not necessarily mutually exclusive. The Geochemical characteristics of these rocks suggest that the deposit is possibly related to mantle derived

intraplate magmas that yielded basalts and olivine diabases of alkaline affinity, and quartz diabases of transitional to tholeitic affinity. The deposit was further enhanced by hydrothermal activity with the involvement of sea water which favoured the appropriate conditions for the generation of this unique deposit. Alkali mafic magmas of mantle origin emplaced in a continental intraplate setting would account for the origin of the Mercury deposit of Almadén. The IRB (Carbonell et al., 2004; Simancas et al., 2003) was located within the OMZ and it appears not to extend towards the CIZ. The ALCUDIA transect does not show evidence of the IRB extending further to the north. Some of the fractures and faults within form the structure underlying the Almadén district, as suggested by the seismic image, could have provided the tectonic link with lower crust and mantle, together with the pathways for the alkaline basaltic magma during the Late Ordovician to Early Devonian. The mineralization was then farther emphasized by the plume activity in Lower Carboniferous.

The relatively high amplitude reflection fabric within the CIZ is localized within the mid-lower crust. This reflection fabric suggests a strongly laminated lower crust which is almost horizontal and limited by a remarkably horizontal Moho located at 31 km depth. The Bouguer anomaly (Figs. 1e and 3c) along the ALCUDIA transect features a 40 mgal difference between the maxima near the southern end of the transect and the minima near the northern end of the transect (García-Lobón et al., 2014). The average topography is 500 m and its high points are located at CDP 11,500 offset to the south of where the relative Bouguer anomaly minimum is located. This 40 mgal decrease in the Bouguer gravity anomaly in almost 250 km and the fact that the Moho is horizontal at 31 km depth suggesting that the physical properties of the crust (in particular the density) are changing towards the north. This simple observation suggests that the CIZ crust features higher content in mafic materials towards the south, within the neighbourhood of the proposed flower structure, until CDP 3000 and decreases in mafic content towards the north. Then the gravity anomaly is nearly horizontal ~40 mgal which suggests that the content in mafic materials is nearly constant from CDP 3000 up to CDP 11,000. From the latter location till the northern end of the transect the crust is less mafic. The available geophysical data (Palomeras et al., 2009, 2011; Pous et al., 2011) over the southern end of the CIZ and the OMZ suggests a mafic composition for the mid-lower crust beneath this contact zone.

The ALCUDIA transect corresponds to a northern extension of the IBERSEIS. One of the most outstanding results of the IBERSEIS transect was the imaging, in the middle crust of the OMZ, of the IRB high amplitude reflection body which was interpreted as a layered mafic intrusion (a stack of mafic sills) (Simancas et al., 2003). This suggests that the mafic rocks that intruded the CIZ are mostly located within the mid-lower crust, and mostly towards the south. At this respect, Carboniferous mafic rocks (both plutons and volcanics) exist in the southern end of the CIZ (Fig. 1c), and are common in the OMZ (coherently with the underlying IRB). These magmas, most probably used the preexisting fault/fracture zones as pathways resulting in a strongly reflecting laminated lower crust. The intrusion of the mafic material affected mostly the flower structure, itself, and decreased to the north. Within the flower structure, Zone I, the attitude of the fractures would be subvertical. This geometry is difficult to image by normal incidence deep seismic reflection data and only patches of reflecting bodies (relatively large boudins) are imaged (Heinonen et al., 2012). The rest corresponds to diffractions and back scattered energy typical seismic images of the crystalline terranes. At increasing distances from the suture zone the attitude of the weak zones (fractures, faults, and shear) is more horizontal favouring the intrusion of sill-like structures, or alternatively as the distance from the interpreted flower structure increases the horizontal fabric could represent anastomosing, ductile shear zones. These would be responsible for the interpreted laminated lower crust.

The Moho discontinuity imaged over the CIZ features relatively high amplitudes and horizontal band of reflectivity. The geometry of Moho over the OMZ shows horizontal to flat reflections (Figs. 3d and 4a). The horizontal geometry of the Moho discontinuity is an important observation as it is located at the same depth, at c. 31 km, along the IBERSEIS (Simancas et al., 2003) and the ALCUDIA transects (Martínez-Poyatos et al., 2012; Simancas et al., 2013). This observation indicates that the southern part of the Iberian Peninsula features a Moho at a constant depth of 30 km from the Gulf of Cadiz to Toledo (Carbonell et al., 2013; Diaz and Gallart, 2009). Therefore, the topography along the ALCUDIA transect characterized by undulating long wavelength (hundreds of km) contrasts with the lack of depth variations for the Moho discontinuity. The topography can change along the ALCUDIA, approximately 0.5 km in average, and in the context of the Iberian Plateau this topographic change can reach 0.7 km. Lithospheric scale folding (Casas-Sainz and De Vicente, 2009; Cloetingh et al., 2002; De Vicente and Vegas, 2009) can account for the long wavelength undulating topography and generated differential uplift/subsidence in the different areas of the Iberian plate. However, the horizontal geometry of the Moho requires that the deformation that resulted in the surface topography needs to be accommodated within the crust by the appropriate structures and or processes. The seismic image strongly supports the partition of the strain in three different ways which are regulated by the rheology and the physical properties (of temperature and pressure). Near the surface and above 10–12 km the deformation appears to be accommodated mostly by folding. These folds are possibly cored by blind thrust which also accommodated some amount of deformation. The faults constitute the limits of upper crustal blocks which move mostly out of the plane of the image and also contribute to the elevation to a small degree. The brittle to ductile transition is the base of this block where the mid-lower crust is probably represented by pods, boudins of material limited by shear zones. These shear zones can be partially intruded by alkali mafic sills which make them more reflective. This structure would be able to accommodate compression by distributed amount of topographic uplift, generating relatively long wavelength folding (Fig. 10). On the ALCUDIA stack section the presence of the subhorizontal tectonic units indicates lateral velocity variations which were not considered in case of the poststack migration. An accurate estimation of velocity model is required to run prestack migration to deal with sharp velocity variations (Flecha et al., 2010). Prestack time migration (Kirchhoff) was applied on the ALCUDIA profile but it did not provide better resolution.

6. Conclusions

In this study, we revised the processing using an improved workflow for the ALCUDIA normal incidence deep seismic profile about 230 km long over an intracontinental part of the western European Variscan Orogen in the Central Iberian Zone (central Spain). The reassessment of the data enabled us to provide a high quality image and led us to an updated and more confident geological interpretation. An optimal estimation of the stacking velocity combined with a good estimation of residual static, refraction static corrections, filtering and migration was the most important processing step.

Although the geology is complex, the image shows much of the shallow and deep structure of the CIZ, as well as the deep structure of the suture with the OMZ. The regions of significant faulting and folding have been presented and interpreted in details along the ALCUDIA profile. The seismic response of the subsurface can be differentiated mainly in two patterns, reflective or transparent. The contacts between the reflective and transparent packages are interpreted as faults and in some cases to originate from lithological variations. The transparent sequences are interpreted to be originated from granitic bodies such as Mora Pluton and Pedroches Batholith, each c. 3.5 km thick. In the upper crust, the tectonic style of deformation is accommodated mainly by folding, high angle faulting and the imbricate thrust systems. In the north, the Toledo Fault and the Mora Fault are imaged as low angle extensional listric features dipping to the south. In the south, the north dipping Central Unit, associated with the CIZ/OMZ suture abuts

Please cite this article as: Ehsan, S.A., et al., Crustal deformation styles along the reprocessed deep seismic reflection transect of the Central Iberian Zone (Iberian Peninsula), Tectonophysics (2014), http://dx.doi.org/10.1016/j.tecto.2014.02.014

against the Espiel thrust. A decollement is defined at c. 13 km, based on the contrast in reflectivity between the upper and the mid-lower crust. Moreover, the occurrence of imbricate thrusts, in the upper crust, shallowing downward implies that they sole down into a subhorizontal basal detachment. The seismic image demonstrates that the upper and mid-lower crust responded differently to the deformation. The reflectivity of the lower crust is typical of the continental crust, dense and subhorizontal to flat across Zone II of the ALCUDIA. However, intense deformation patterns are recognized as transpression/thrusting across Zone I and III of the image. The ALCUDIA profile shows dipping reflections wedging into the upper mantle that are interpreted to represent the Tomar–Badajoz–Cordoba shear zone at depth. The Moho discontinuity is imaged at c. 31 km depth as flat lying reflections with minor undulations.

Acknowledgements

Seismic data were collected in 2007 with funding provided by the Spanish Ministry of Science and Innovation (grants: CGL2004-04623/BTE, CGL2007-63101/BTE, CGL2011-24101, CSD2006-00041) and the Junta de Castilla-La Mancha. S.A. Ehsan is funded by the European Commission grant Marie Curie Actions (264517-TOPOMOD-FP7-PEOPLE-2010-ITN). We thank Instituto Geológico y Minero de España for providing the logistic help and an academic crew for the data acquisition. Ignacio Marzan, Alireza Malehmir, Peter Hedin, Dennis Brown and Giovanni Camanni are acknowledged for the valuable suggestions. We appreciate the useful reviews by Ron Clowes, an anonymous reviewer that helped to improve the manuscript. GLOBE Claritas™ under license from the Institute of Geological and Nuclear Sciences Limited, Lower Hutt, New Zealand was used to process the seismic data. GMT was used to prepare some of the figures shown in the paper.

References

Aranguren, A., Larrea, F.J., Carracedo, M., Cuevas, J., Tubia, J.M., 1997. The Los Pedroches batholith (southern Spain): polyphase interplay between shear zones in transtension and setting of granites. Granite: From Segregation of Melt to Emplacement FabricsKluwer Academic Publishers, Dordrecht 215–229.

Azor, A., González Lodeiro, F., Simancas, J.F., 1994. Tectonic evolution of the boundary between the Central Iberian and Ossa–Morena zones (Variscan Belt, SW Spain). Tectonics 13, 45–61. http://dx.doi.org/10.1029/93TC02724.

Barbero, L., 1995. Granulite-facies metamorphism in the Anatectic Complex of Toledo, late Hercynian tectonic evolution by crustal extension. J. Geol. Soc. Lond. 152, 365–382.

Boorder, H., Westerhof, A.B., 1994. Tectonic control of early to middle Paleozoic volcanism and related mercury and antimony mineralization in southern central Iberia. Econ. Geol. 89, 656–661. http://dx.doi.org/10.2113/gsecongeo.89.3.656.

Burg, J.P., Iglesias, M., Laurent, P., Matte, P., Ribeiro, A., 1981. Variscan intracontinental deformation: the Coimbra–Córdoba Shear Zone (SW Iberian Peninsula). Tectonophysics 78, 161–177. http://dx.doi.org/10.1016/0040-1951(81)90012-3.

Carbonell, R., Pérez-Estaún, A., Gallart, J., Díaz, J., Kashubin, S., Mechie, J., Stadtlander, R., Schulze, A., Knapp, J.H., Morozov, A., 1996. Crustal root beneath the Urals: wide-angle seismic evidence. Science 274, 222–224. http://dx.doi.org/10.1126/science.274.5285.222.

Carbonell, R., Lecerf, D., Itzin, M., Gallart, J., Brown, D., 1998. Mapping the Moho beneath the southern Urals with wide-angle reflections. Geophys. Res. Lett. 25, 4229–4232. http://dx.doi.org/10.1029/1998GL900107.

Carbonell, R., Gallart, J., Pérez-Estaún, A., Díaz, J., Kashubin, S., Mechie, J., Wenzel, F., Knapp, J.H., 2000. Seismic wide-angle constraints on the crust of the southern Urals. J. Geophys. Res. 105, 13755–13777. http://dx.doi.org/10.1029/2000JB900048.

Carbonell, R., Simancas, J.F., Juhlin, C., Pous, J., Pérez-Estaún, A., González Lodeiro, F., Muñoz, G., Heise, W., Ayarza, P., 2004. Geophysical evidence of a mantle derived intrusion in SW Iberia. Geophys. Res. Lett. 31, L11601. http://dx.doi.org/10.1029/2004GL019684.

Carbonell, R., Levander, A., Kind, R., 2013. The Mohorovičič discontinuity beneath the continental crust: an overview of seismic constraints. Tectonophysics 609, 353–376. http://dx.doi.org/10.1016/j.tecto.2013.08.037.

Casas-Sainz, A.M., Cortés-Gracia, A.L., 2002. Cenozoic landscape development within the Central Iberian Chain, Spain. Geomorphology 44, 19–46.

Casas-Sainz, A.M., de Vicente, G., 2009. On the tectonic origin of Iberian topography. Tectonophysics 474, 214–235. http://dx.doi.org/10.1016/j.tecto.2009.01.030.

Casas-Sainz, A.M., Faccenna, C., 2001. Tertiary compressional deformation of the Iberian plate. Terra Nova 13, 281–288. http://dx.doi.org/10.1046/j.1365-3121.2001.00355.x.

Cheraghi, S., Malehmir, A., Bellefleur, G., 2011. Crustal-scale reflection seismic investigations in the Bathurst Mining Camp, New Brunswick, Canada. Tectonophysics 506, 55–72. http://dx.doi.org/10.1016/j.tecto.2011.04.11.

Cloetingh, S., Burov, E., Beekman, F., Andeweg, B., Andriessen, P.A.M., Garcia-Castellanos, D., de Vicente, G., Vegas, R., 2002. Lithospheric folding in Iberia. Tectonics 21, 1–26. http://dx.doi.org/10.1029/2001TC901031.

Deregowski, S.M., 1986. What is DMO? First Break 4, 7–24.

De Vicente, G., Vegas, R., 2009. Large-scale distributed deformation controlled topography along the western Africa–Eurasia limit: tectonic constraints. Tectonophysics 474, 124–143. http://dx.doi.org/10.1016/j.tecto.2008.11.026.

Diaz, J., Gallart, J., 2009. Crustal structure beneath the Iberian Peninsula and surrounding waters: a new compilation of deep seismic sounding results. Phys. Earth Planet. Inter. 173, 181–190.

Doblas, M., et al., 1994. Extensional tectonics in the central Iberian Peninsula during the Variscan to Alpine transition. Tectonophysics 238, 95–116.

Echtler, H.P., Stiller, M., Steinhoff, F., Krawczyk, C., Suleimanov, A., Spiridonov, V., Knapp, J. H., Menshikov, Y., Alvarez-Marron, J., Yunusov, N., 1996. Preserved collisional crustal structure of the southern Urals revealed by vibroseis profiling. Science 274, 224–226.

Flecha, I., Carbonell, R., Hobbs, R.W., Zeyen, H., 2010. Some improvements in subbasalt imaging using pre-stack depth migration. Solid Earth Discuss. 2, 1–17. http://dx.doi.org/10.5194/sed-2-1-2010.

Franke, W., 2000. The mid-European segment of the Variscides: tectonostratigraphic units, terrane boundaries and plate tectonic evolution. Geol. Soc. Spec. Publ. 179, 35–61. http://dx.doi.org/10.1144/GSL.SP.2000.179.01.05.

Freeman, B., Klemperer, S.L., Hobbs, R.W., 1988. The deep structure of northern England and the Iapetus Suture zone from BIRPS deep seismic reflection profiles. J. Geol. Soc. Lond. 145, 727–740.

Friberg, M., Juhlin, C., Beckholmen, M., Petrov, G.A., Green, A.G., 2002. Palaeozoic tectonic evolution of the Middle Urals in the light of the ESRU seismic experiments. J. Geol. Soc. 159, 295–306.

García-Lobón, J.L., Rey-Moral, C., Ayala, C., Martín-Parra, L.M., Matas, J., Reguera, M.I., 2014. Regional structure of the southern segment of Central Iberian Zone (Spanish Variscan Belt) interpreted from potential field images and 2.5 D modelling of Alcudia gravity transect. Tectonophysics 614, 185–202. http://dx.doi.org/10.1016/j.tecto.2013.12.005.

Hall, C.M., Higueras, P.L., Kesler, S.E., Lunar, R., Hailing, D., Halliday, A.N., 1997. Dating of alteration episodes related to mercury mineralization in the Almadén district, Spain. Earth Planet. Sci. Lett. 148, 287–298. http://dx.doi.org/10.1016/S0012-821X(97)00041-1.

Heinonen, S., Imaña, M., Snyder, D., Kukkonen, I., Heikkinen, P., 2012. Seismic reflection profiling of the Pyhäsalmi VHMS-deposit: a complementary approach to the deep base metal exploration in Finland. Geophysics 77, 15–23. http://dx.doi.org/10.1190/geo2011-0240.1.

Heinonen, S., Heikkinen, P.J., Kousa, J., Kukkonen, I.T., Snyder, D.B., 2013. Enhancing hardrock seismic images: reprocessing of high resolution seismic reflection data from Vihanti, Finland. J. Appl. Geophys. 93, 1–11. http://dx.doi.org/10.1016/j.jappgeo.2013.03.004.

Heinze, W., Loeschke, J., Vavra, G., 1985. Phreatomagmatic volcanism during the Ordovician of the Cantabrian Mountains. Geol. Rundsch 74, 623–639.

Hernandez, A.M., 1984. Estructura y génesis de los yacimientos demercurio de Almadén. (PhD Thesis) University of Salamanca.

Hernàndez-Enrile, J.L., 1991. Extensional tectonics of the Toledo ductile–brittle shear zone, central Iberian Massif. Tectonophysics 191, 311–324.

Higueras, P., Oyarzun, R., Munha, J., Morata, D., 2000. Palaeozoic magmatic-related hydrothermal activity in the Almadén syncline (Spain): a Silurian–Devonian persistent process? Trans. Inst. Min. Metall. 109, 199–202.

Jebrak, M., Higueras, P.L., Marcoux, E., Lorenzo, S., 2002. Geology and geochemistry of high-grade, volcanic rock-hosted, mercury mineralisation in the Nuevo Entredicho deposit, Almadén district, Spain. Mineral. Deposita 37, 421–432. http://dx.doi.org/10.1007/s00126-001-0222-y.

Juhlin, C., Friberg, M., Echtler, H.P., Hismatulin, T., Rybalka, A., Green, A.G., Ansorge, J., 1998. Crustal structure of the middle Urals: results from the ESRU experiments. Tectonics 17, 710–725. http://dx.doi.org/10.1029/98TC02762.

Juhlin, C., Dehghannejad, M., Lund, B., Malehmir, A., Pratt, G., 2010. Reflection seismic imaging of the end-glacial Pärvie Fault system, northern Sweden. J. Appl. Geophys. 70, 307–316. http://dx.doi.org/10.1016/j.jappgeo.2009.06.004.

Klemperer, S.L., Matthews, D.H., 1987. Iapetus Suture located beneath the North Sea by BIRPS deep seismic reflection profiling. Geology 15, 195–198.

Malehmir, A., Juhlin, C., 2010. An investigation of the effects of the choice of stacking velocities on residual statics for hardrock reflection seismic processing. J. Appl. Geophys. 72, 28–38. http://dx.doi.org/10.1016/j.jappgeo.2010.06.008.

Martínez-Poyatos, D., et al., 2012. Imaging the crustal structure of the Central Iberian Zone (Variscan Belt): the ALCUDIA deep seismic reflection transect. Tectonics 31, TC3017. http://dx.doi.org/10.1029/2011TC002995.

Matte, P., 1986. Tectonics and plate tectonics model for the Variscan Belt of Europe. Tectonophysics 126, 329–374.

Matte, P., 2001. The Variscan collage and orogeny (480–290 Ma) and the tectonic definition of the Amorica microplate: a review. Terra Nova 13, 122–128. http://dx.doi.org/10.1046/j.1365121.2001.00327.x.

Maucher, A., 1976. The Stratabound Cinnabar–Stibnite–Scheelite Deposits (Discussed with Examples from the Mediterranean Region). Handbook of Strata-Bound and Stratiform Ore Deposits. Elsevier, Amsterdam Oxford-New York.

Onken, O., Plesh, A., Weber, J., Ricken, W., Schrader, S., 2000. Passive margin detachment during arc-continent collision (central European Variscides), in orogenic processes: quantification and modelling in the Variscan Belt. Geol. Soc. Spec. Publ. 179, 9–20.

Ortega, E., 1986. Geology and metallogeny of the Almaden area, Centro-Iberian zone, Spain. European Workshop on Remote Sensing 2nd Brussels Proceedings, pp. 148–173.

Ortega, E., Hernandez, A., 1992. The mercury deposits of the Almadén syncline, Spain. Chronique de la Recherche Miniere 506, 3–24.

Please cite this article as: Ehsan, S.A., et al., Crustal deformation styles along the reprocessed deep seismic reflection transect of the Central Iberian Zone (Iberian Peninsula), Tectonophysics (2014), http://dx.doi.org/10.1016/j.tecto.2014.02.014

Palomeras, I., Carbonell, R., Flecha, I., Simancas, J.F., Ayarza, P., Matas, J., Martínez-Poyatos, D., Azor, A., González Lodeiro, F., Pérez-Estaún, A., 2009. Nature the lithosphere across the Variscan orogen of SW Iberia: dense wide-angle seismic reflection data. J. Geophys. Res. 114, B02302. http://dx.doi.org/10.1029/2007JB005050.

Palomeras, I., Carbonell, R., Ayarza, P., Fernandez, M., Simancas, J.F., Martínez-Poyatos, D., González Lodeiro, F., Pérez-Estaún, A., 2010. Geophysical model of the lithosphere across the Variscan Belt of SW-Iberia: multidisciplinary assessment. Tectonophysics 508, 42–51. http://dx.doi.org/10.1016/j.tecto.2010.07.010.

Palomeras, I., Carbonell, R., Ayarza, P., Martí, D., Brown, D., Simancas, J.F., 2011. Shear wave modeling and Poisson's ratio in the Variscan Belt of SW Iberia. Geochem. Geophys. Geosyst. 12, Q07008. http://dx.doi.org/10.1029/2011GC003577.

Peabody, C.E., Einaudi, M.T., 1992. Origin of petroleum and mercury in the Culver–Baer cinnabar deposit, Mayacmas District, California. Econ. Geol. 87, 1078–1103. http://dx.doi.org/10.2113/gsecongeo.87.4.1078.

Pérez-Estaún, A., Bea, F. (Eds.), 2004. Macizo Ibérico. En: Geología de España (J.A. Vera, Ed.). Soc. Geol. España; Inst. Geol. Min., España, Madrid, pp. 19–230.

Pirajno, F., 2010. Intracontinental strike-slip faults, associated magmatism, mineral systems and mantle dynamics: examples from NW China and Altay–Sayan (Siberia). J. Geodyn. 50, 325–346. http://dx.doi.org/10.1016/j.jog.2010.01.018.

Pous, J., et al., 2011. Constraints on the crustal structure of the internal Variscan Belt in SW Europe: a magnetotelluric transect along the eastern part of Central Iberian Zone, Iberian Massif. J. Geophys. Res. 116, 1–20. http://dx.doi.org/10.1029/2010JB007538.

Robinson, S.E., Coruh, C., 1988. Basic Exploration Geophysics. Virginia Polytechnic institute and State University.

Rosenbaum, G., Lister, G.S., Duboz, C., 2002. Relative motions of Africa, Iberia and Europe during Alpine orogeny. Tectonophysics 359, 117–129. http://dx.doi.org/10.1016/S0040-1951(02)00442-0.

Saupe, F., 1990. Geology of the Almadén mercury deposit, Province of Ciudad Real, Spain. Econ. Geol. 85, 482–510.

Schmelzbach, C., Juhlin, C., Carbonell, R., Simancas, J.F., 2007. Prestack and poststack migration of crooked-line seismic reflection data: a case study from the South Portuguese Zone fold belt, southwestern Iberia. Geophysics 72, 9–18. http://dx.doi.org/10.1190/1.240 7267.

Simancas, J.F., Martínez-Poyatos, D., Exposito, I., Azor, A., Gonzalez Lodeiro, F., 2001. The structure of a major suture zone in the SW Iberian Massif: the Ossa–Morena/Central Iberian contact. Tectonophysics 332, 295–308.

Simancas, J.F., et al., 2003. The crustal structure of the transpressional Variscan Orogen of the SW Iberia: the IBERSEIS deep seismic reflection profile. Tectonics 22, 1062. http://dx.doi.org/10.1029/2002TC001479.

Simancas, J.F., Ayarza, P., Azor, A., Carbonell, R., Martínez-Poyatos, D., Pérez-Estaún, A., González Lodeiro, F., 2013. A seismic geotraverse across the Iberian Variscides: orogenic shortening, collisional magmatism, and orocline development. Tectonics 32, 417–432. http://dx.doi.org/10.1002/tect.20035.

Tejero, R., González-Casado, J.M., Gómez-Ortiz, D., Sánchez-Serrano, F., 2006. Insights into the "tectonic topography" of the present-day landscape of the central Iberian Peninsula (Spain). Geomorphology 76, 280–294. http://dx.doi.org/10.1016/j.geomorph.2005.11.007.

Tryggvason, A., Brown, D., Pérez-Estaún, A., 2001. Crustal architecture of the southern Uralides from true amplitude processing of the URSEIS vibroseis profile. Tectonics 20, 1040–1052.

Verges, J., Fernandez, M., 2006. Ranges and basins in the Iberian Peninsula: their contribution to the present topography. J. Geol. Soc. Lond. 32, 223–234.

Vollbrecht, A., Weber, K., Schmoll, J., 1989. Structural model for the Saxothuringian–Moldanubian suture in the Variscan basement of the Oberpfalz (Northeastern Bavaria, F.R.G.) interpreted from geophysical data. Tectonophysics 157, 123–133. http://dx.doi.org/10.1016/0040-1951(89)90346-6.

White, D., Boerner, D., Wu, J., Lucas, S., Berrer, E., Hannila, J., Somerville, R., 2000. Mineral exploration in the Thompson nickel belt, Manitoba, Canada using seismic and controlled-source EM-methods. Geophysics 65, 1871–1881. http://dx.doi.org/10.1190/1.1444871.

Yilmaz, Ö., 1989. Seismic Data Processing: Investigations in Geophysics. SEG.

Yilmaz, Ö., 2001. Seismic Data Analysis: Processing, Inversion and Interpretation of Seismic Data. SEG.

Zengqian, H., Hongwen, M., Zaw, K., Yuquan, Z., Mingjie, W., Zeng, W., Guitang, P., Renli, T., 2003. The Himalayan Yulong porphyry copper belt: product of large-scale strike-slip faulting in Eastern Tibet. Econ. Geol. 98, 125–145.

Please cite this article as: Ehsan, S.A., et al., Crustal deformation styles along the reprocessed deep seismic reflection transect of the Central Iberian Zone (Iberian Peninsula), Tectonophysics (2014), http://dx.doi.org/10.1016/j.tecto.2014.02.014